residues on the template strand without halting DNA synthesis. Furthermore, the B-family DNA pol from *S. solfataricus* (Sso DNA pol B1) was reported to recognize the presence of hypoxanthine in the template, in addition to uracil, and to stall synthesis 3–4 bases upstream of this lesion (Gruz et al. 2003). Stalling of Sso DNA pol B1 at the template uracil has been also visualized by atomic force microscopy (Asami et al. 2006). The "read-ahead" function of the archaeal hyper-thermophilic B-family DNA pols is likely to operate as an additional safeguard mechanism against increased level of deaminated bases in the template DNA strand during genome duplication at high temperature. Analysis of the X-ray crystal structure of some archaeal B-family DNA pols revealed the presence of a special binding pocket for the uracil in the extreme N-terminal portion and site-specific mutagenesis studies confirmed this structural prediction for the B-family DNA pol of *Pyrococcus furiosus* (Fogg et al. 2002).

Interestingly, crenarchaea from the genus *Sulfolobus* possess a DNA pol belonging to the Y-family, in addition to the B-family enzyme (Kulaeva et al. 1996; Gruz et al. 2001). A peculiar feature of Y-family DNA pols is their ability to bypass various lesions in template DNA in an error-prone or error-free manner (Wang 2001; Freidberg et al. 2002). Thus, this family of DNA polymerases plays a critical role in genome stability in bacterial and eukaryotic organisms. Y-family DNA pols from *Sulfolobales* are extremely interesting enzymes since the X-ray structure of two of them (*S. acidocaldarius* and *S. solfataricus*) has been solved providing important structural information about the DNA lesion bypass mechanism (Ling et al. 2001; Silvian et al. 2001; Zhou et al. 2001). The Y-family DNA polymerase from *S. solfataricus* (Sso DNA pol Y1) has been reported to bypass a variety of DNA lesions (Gruz et al. 2001) and to catalyze erroneous incorporation of oxidized dNTPs (such as 8-OH-dGTP and 2-OH-dATP) into nascent DNA (Shimizu et al. 2003).

Herein we report evidence that Sso DNA pol B1 physically interacts with DNA pol Y1 by surface plasmon resonance measurements and immuno-precipitation experiments. The region responsible for this interaction has been mapped in the central portion of DNA pol B1 polypeptide chain (from the amino acid residue 482 to 617). The results of this analysis have important implications for understanding genome stability mechanisms in the hyper-thermophilic crenarchaeon *S. solfataricus*.

Materials and methods

Proteins

His-tagged Sso DNA pol B1 and the DNA pol Y1 were purified from *E. coli* over-expressing strains as described by Lou et al. (2004) and by Shimizu et al. (2003), respectively.

The truncated forms of Sso DNA pol B1 were produced by PCRs using the pET-DNA pol B1 plasmid DNA as the template. To produce the proteins Sso DNA pol B1-721, -617 and -481 the 5′-primer, named Nt-*Bam*, had the following sequence: 5′-GGGTTT GGATCCGAATGACTAAGCAACTTACCTTA-3′, the *Bam*H1 restriction site is underlined; the 3′-primers were respectively: B-721-*Hin*d (5′-TTGGAAGCTTCTATG TTTCAGTCCAAATACACCGTA-3′); B-617-*Hin*d (5′-TTGGAAGCTTCTATCTCTTCTTCACTAACATCC CCTT-3′); B-481-*Hin*d (5′-GGGTTTAAGCTTCTATT TCGCTAAGATTTCTTCCTT-3′). These latter oligonucleotides contain a stop codon immediately upstream the *Hin*dIII restriction site. The PCR amplified DNA fragment were purified, digested with *Bam*HI and *Hin*dIII and cloned into the *E. coli* expression vector pTRC-*His*C (Invitrogen). All the cloned DNA fragments were sequenced to rule out the presence of undesired mutations.

To produce the recombinant proteins *E. coli* competent cells of the strain BL21(DE3) Rosetta (Novagen) were transformed with each expression plasmid. Transformed cells were grown in 0.5 litre of LB medium supplemented with chloramphenicol (at 30 μg/ml) and ampicillin (at 100 μg/ml). When the culture reached an optical density of 0.7 unit at 600 nm expression of the recombinant protein was induced by adding IPTG at 0.2 mM into the medium. Then the bacterial culture was incubated at 37°C for additional 2 h. Cells were harvested by centrifugation at 8,000 rpm for 10 min at 10°C using a GS-3 Sorvall rotor. Cell pellets were stored at −20°C until use.

Pellets of *E. coli* recombinant cells expressing the truncated protein Sso DNA pol B1-481 or -721 were resuspended in 10 ml of Buffer A (20 mM Tris–HCl, pH 8.0, 0.1 mM EDTA, 1 mM DTT, 50 mM NaCl) containing protease inhibitors (PMSF at 50 μg/ml, benzamidine at 0.2 μg/ml, aprotinin at 1 μg/ml). Cells were lysed by two consecutive passages through a French press apparatus (Aminco Co., Silver Spring, MD) at 1,500 p.s.i.. The cell extract was centrifuged at 30,000 rpm for 30 min at 10°C in a Beckman 70.0 Ti rotor. The supernatant was incubated at 70°C per 15 min and transferred into ice per 10 min. The heat-treated samples were centrifuged at 30,000 rpm for 30 min at 10°C in a Beckman 70.0 Ti rotor. The supernatants, filtered through a 0.22 μm filter, were loaded onto a Ni^{2+}-NTA chelate agarose super-flow column (Qiagen) equilibrated in Buffer A. Bound proteins were eluted by a stepwise gradient of imidazole (10–500 mM) in Buffer A containing 20% glycerol. Collected fraction (1 ml) were analysed by SDS-PAGE and those containing the recombinant protein were pooled and dialysed against Buffer B (20 mM Tris–HCl, pH 8.0, 1 mM DTT, 200 mM NaCl) overnight at 10°C. The sample was concentrated and stored at −20°C.

Pellets of *E. coli* recombinant cells expressing the truncated protein Sso DNA pol B1-617 were treated as described before. The cell extract was incubated for 10 min at 65°C and then transferred to ice for 10 min. The sample was centrifuged at 30,000 rpm for 30 min

using a Beckman 70.0 Ti rotor. The supernatant was filtered through a 0.22 μm filter and subjected to anionic-exchange chromatography on a Mono Q HR 10/10 column (Amersham/Pharmacia Biosciences) equilibrated in Buffer A. The column was developed with a linear gradient of NaCl (0–1 M). Collected fractions (1 ml) were analysed by SDS-PAGE and those containing the recombinant protein were pooled. The sample was dialysed against Buffer C (10 mM Tris–HCl, pH 8.5, 2.5 mM $MgCl_2$) overnight at 10°C and loaded onto a Heparin Sepharose column equilibrated in Buffer C. Fractions containing the recombinant protein were pooled and dialysed against Buffer B overnight at 10°C, concentrated and stored at −20°C.

Surface plasmon resonance measurements

Real-time interactions of Sso DNA pol B1 and DNA pol Y1 were monitored using the surface plasmon resonance biosensor system Biacore 2000 (Biacore). Sso DNA pol B1 was diluted to a concentration of 20 μg/ml in buffer 10 mM sodium acetate pH 3.6 and coupled to the carboxy-methylated dextran modified gold surface of a CM5 sensor chip, according to the manifacturer's instruction manual. Sso DNA pol Y1 was diluted at 40 μg/ml in buffer 10 mM sodium acetate pH 5.0 and immobilised using the same procedure. Under these conditions, surfaces containing densities of about 2,100 resonance units of Sso DNA pol B1 and 7,000 resonance units of Sso DNA pol Y1 were generated. To collect sensorgrams the indicated proteins at various concentrations were passed over the sensor surface at a flow rate of 10 μl/min. Recorded sensorgrams were normalised to a baseline of zero resonance unit and analysed using the BIA Evaluation software.

Immuno-precipitation experiments

Protein A Sepharose CL-4B resin (250 μg) was re-suspended in Binding Buffer (50 mM Tris–HCl pH 7.0, 40 mM NaCl, 20 mM $MgCl_2$, 2.5 mM 2-mercaptoethanol) and conjugated with anti-Sso DNA pol Y1 antibodies. Mixtures (final volume: 40 μl) were prepared which contained in Binding Buffer: 9 μg of Sso DNA pol B1 and 7 μg of Sso DNA pol Y1, 9 μg of Sso DNA pol B1 alone (negative control experiment), 7 μg of Sso DNA pol Y1 alone (positive control experiment). To each mixture 80 μl of Protein A Sepharose resin conjugated with anti-Sso DNA pol Y1 antibodies were added. The samples were incubated for 1 h at room temperature with gentle shaking. The resin of each mixture was washed with 5 ml of Washing Buffer (50 mM Tris–HCl pH 7.0, 300 mM NaCl, 1 mM $MgCl_2$, 1% Triton-X-100) and then re-suspended in 60 μl of SDS-PAGE Sample Buffer 1× (62 mM Tris–HCl pH 6.8, 1% glycerol, 0.5% SDS, 0.5% 2-mercapto-ethanol, 0.01% blue bromophenol). Samples were run on a 10% polyacrylamide denaturing gel. After the electrophoretic run the gel was transferred to a PVDF membrane, which was cut into two halves: the upper part was analysed using anti-His antibodies conjugated with horseradish peroxidase (Qiagen) and the ECL + system (Amersham/Pharmacia Biosciences). The lower half of the membrane was analysed using anti-Sso DNA polY1 antibodies and the anti-rabbit IgG antibodies conjugated with alkaline phosphatase as the primary and secondary antibody, respectively.

Results

Direct physical interaction between Sso DNA pol B1 and DNA pol Y1

The physical interaction between Sso DNA pol B1 and DNA pol Y1 was monitored using the surface plasmon resonance Biacore 2000 system. In an initial set of experiments Sso DNA pol B1 solutions of increasing concentrations were passed over a DNA pol Y1-immobilised CM5 sensor chip. Fig. 1 shows an example of overlaid sensorgrams obtained with four different concentrations of DNA polB1 (from 0.15 to 1.2 μM). The amplitude of the curves is proportional to the concentration of the analyte, suggesting a direct physical association of the two proteins. The dissociation rate of DNA pol B1 was very low and the equilibrium dissociation constant (K_D) was in the order of 1×10^{-8} M. Evidence for a physical interaction between the two *Sulfolobus* DNA pols was obtained in similar experiments where DNA pol Y1 was used as the analyte and DNA pol B1 as the ligand (data not shown).

The Sso DNA pol B1/DNA pol Y1 interaction was also tested by immuno-precipitation experiments using the purified recombinant proteins. Protein A Sepharose beads conjugated with anti-DNA pol Y1 antibodies were added to mixtures of the two polymerases. As shown in Fig. 2, DNA pol B1 was pulled down with

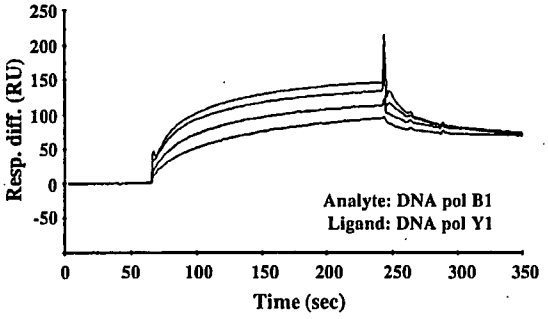

Fig. 1 Physical interaction between Sso DNA pol B1 and DNA pol Y1 detected by surface plasmon resonance measurements. An overlaid plot of sensorgrams was obtained by fluxing DNA pol B1 at various concentrations over a DNA pol Y1-immobilised sensor chip (*lower to upper curve* DNA pol B1 was at 0.15, 0.3, 0.6 and 1.2 μM, respectively), as described in Materials and methods

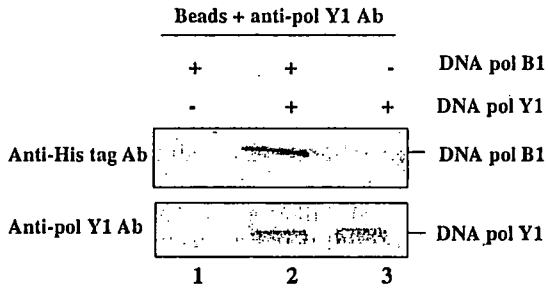

Fig. 2 Physical interaction between Sso DNA pol B1 and DNA pol Y1 detected by immuno-precipitation experiments. Immuno-precipitation experiments were carried out using Protein A Sepharose beads conjugated with anti-DNA pol Y1 antibodies. The following protein samples were analysed: *lane 1*, Sso DNA pol B1 alone (9 μg, negative control experiment); *lane 2*, a mixture of Sso DNA pol B1 (9 μg) and Sso DNA pol Y1 (7 μg); *lane 3*, Sso DNA pol Y1 alone (7 μg, positive control experiment). After the electrophoretic run the gel was transferred to a PVDF membrane, which was cut into two halves: the upper part was analysed using anti-His antibodies using the ECL+ system to detect the His-tagged Sso DNA pol B1. The lower half of the membrane was analysed using anti-Sso DNA polY1 antibodies and the anti-rabbit IgG antibodies conjugated with alkaline phosphatase as the primary and secondary antibody, respectively

DNA pol Y1 in these experiments confirming that a physical association takes place between the two proteins, as also indicated by the surface plasmon resonance analyses.

Production of Sso DNA pol B1 truncated forms

In previous studies we demonstrated that the Sso DNA pol B1 possesses a modular organization with regions that are hyper-sensitive to the proteolytic digestion (Pisani and Rossi 1994; Pisani et al. 1996). The resolution of the Sso DNA pol B1 crystallographic structure by X-ray diffraction analysis confirmed the domain organization of the protein (Savino et al. 2004). Based on this knowledge, we designed truncated forms of DNA pol B1 with the aim of identifying the protein region responsible for the physical interaction with DNA pol Y1 (see Fig. 3). The DNA pol B1-721 deleted protein lacks the whole "thumb" sub-domain (residues 721–882) which is responsible for the interaction with the DNA template strand. The truncated form DNA pol B1-617 lacks almost the entire polymerase module, excluding a small portion of the "palm" sub-domain (the beta-sheets 19–21 and the alpha-helix Q) and the "fingers" sub-domain. The truncated protein DNA pol B1-481 consisted of the protein N-terminal half including the uracil-binding pocket and the proof-reading exonuclease domain. These three C-terminally deleted forms of DNA pol B1 were produced in *E. coli* as *His*-tagged proteins using the pTRC-*His* vector system and found to be soluble. Their purification was readily attained by heat-treatment of the cell extracts and chromatographic procedures (see Fig. 3).

Interaction of the Sso DNA pol B1 truncated forms with the DNA pol Y1

The physical interaction of the Sso DNA pol B1 deleted forms with DNA pol Y1 was probed by surface plasmon resonance measurements. In these experiments solutions of each purified protein of various concentrations were passed over a DNA pol Y1-immobilised CM5 sensor chip. The protein DNA pol B1-481 was unable to interact with DNA pol Y1 suggesting that the C-terminal polymerase domain (residues 482–882) contains the region critical for the interaction with DNA pol Y1.

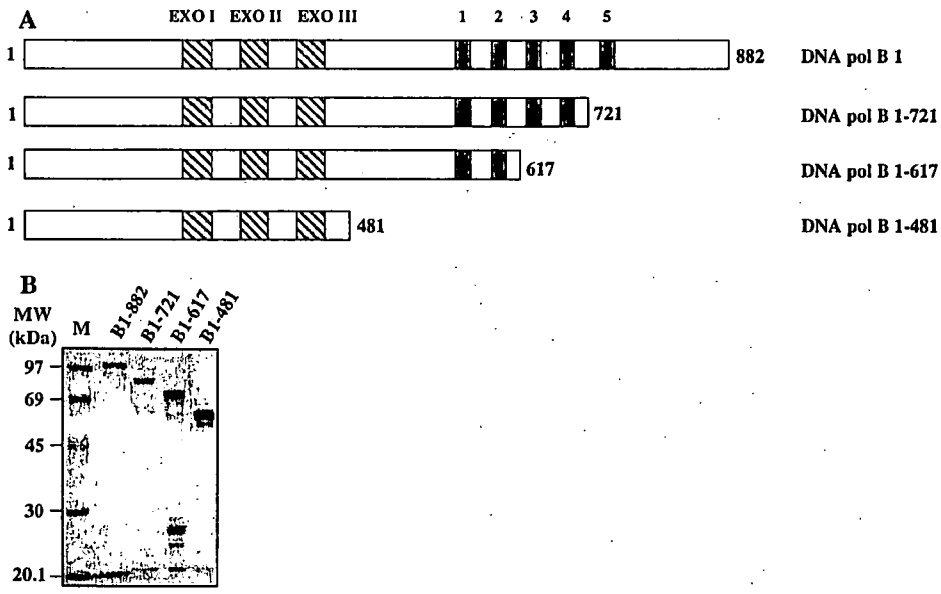

Fig. 3 Diagrammatic representation of Sso DNA pol B1 deleted forms used in this study. **a** The position of the B Family DNA pols sequence similarity motifs is indicated (Blanco et al. 1991). **b** Electrophoretic analysis of purified DNA pol B1 and its deleted forms (5 μg) on a 10% SDS-polyacrylamide gel and Coomassie Blue staining. The molecular weight of size markers run in the *lane M* are reported on the left part of the panel

Surface plasmon resonance measurements were also carried out using either Sso DNA pol B1-617 or -721 truncated proteins as the analytes. Both these truncated forms were found to physically associate with the DNA pol Y1 with a binding affinity comparable with the full-sized DNA pol B1. As shown in Fig. 4, similar sensorgrams were obtained by fluxing each DNA pol B1 C-terminal deleted form over a DNA pol Y1-immobilised sensor chip. These results suggest that the protein region from residue 482 to 617 is critical for the DNA pol B1/DNA pol Y1 interaction.

Discussion

The hyper-thermophilic crenarchaeon *S. solfataricus* has two functional DNA polymerases, DNA pol B1 and DNA pol Y1. We previously reported that these DNA pols are expressed at about the same level in *S. solfataricus* cells by quantitative Western blot analysis suggesting that both enzymes play an important role in genome maintenance (Gruz et al. 2003). Sso DNA pol B1 is able to recognize the deaminated bases uracil and hypoxanthine on the template DNA strand and to stop synthesis 3–4 bases upstream of these lesions. In addition, Sso DNA pol B1 also stops nucleotide incorporation 1 base before 8-oxo-guanine. In contrast, Sso DNA pol Y1 belongs to the family of translesion synthesis DNA pols and readily bypasses all these damaged bases in the template strand. Our analysis has revealed that Sso DNA pol B1 and DNA pol Y1 directly interact in vitro, as assessed by surface plasmon resonance measurements and immuno-precipitation experiments. The results of the protein-protein interaction experiments carried out with the DNA pol B1 truncated forms suggest that the region responsible for this physical interaction spans amino acid residues 482–617. This portion of the Sso DNA pol B1 polypeptide chain includes the extended protease hyper-sensitive linker between the N-and C-terminal modules of the enzyme (amino acid residues Asn482-Ala497) and the α-helices forming the "fingers" sub-domain (α-helices *R*, *R'*and *S*; Savino et al. 2004). The extended linker was demonstrated to be highly flexible and exposed to the solvent in a limited proteolysis study (Pisani et al. 1996) and this notion has been subsequently confirmed by the X-ray crystallographic analysis of Sso DNA pol B1 (Savino et al. 2004). In fact, the 3D structure of this region is not traced in the protein structural model because of its poorly or completely undefined electron density due to high conformational mobility. It is tempting to speculate that interaction with DNA pol Y1 could stabilize this linker region and protect it against the protease attack in vivo.

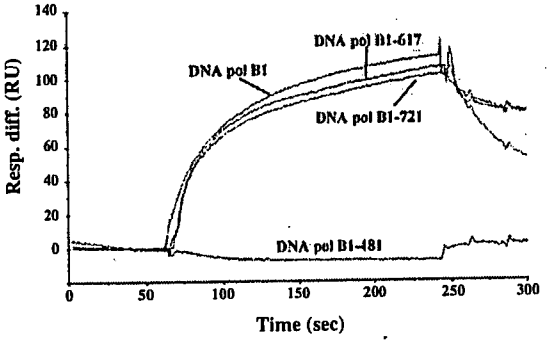

Fig. 4 Physical interaction of the Sso DNA pol B1 truncated forms with DNA pol Y1 detected by surface plasmon resonance measurements. Plot of sensorgrams obtained by fluxing each indicated protein at 0.3 μM over a DNA pol Y1-immobilised sensor chip, as described in Materials and methods

Mouse and human REV1 subunit of DNA pol ζ were reported to physically interact with the trans lesion synthesis DNA pols ι, η and κ and this interaction was proposed to play a pivotal role in the multi-enzyme, multi-step process of lesion bypass in mammal cells (Guo et al. 2003; Ohashi et al. 2004). In *S. solfataricus* cells, stalling of DNA pol B1 at the template uracil or hypoxanthine may generate single strand gap downstream of the lesion site. Gap filling is likely to be carried out by homologous recombination or translesion synthesis by DNA pol Y1. This latter event requires a switch from DNA pol B1 to DNA pol Y1 at the damaged base. Based on the results of our biochemical analysis, we propose that the physical interaction between Sso DNA pol B1 and DNA pol Y1 could play a role in the polymerase switching mechanism at the lesion site during chromosomal replication. However, we were unable to detect any effect on the uracil-bypass efficiency by Sso DNA pol Y1 in the presence of the full-sized DNA pol B1 or its C-terminal truncated forms. It is quite likely that other factors participate in the translesion synthesis process in *S. solfataricus* cells. After lesion bypass by DNA pol Y1, additional DNA repair enzymes might be recruited at the stalled replication fork, such as DNA glycosylases. These enzymes have been identified in various hyper-thermophilic archaea (Sartori and Jiricny 2003; Chung et al. 2003). It has been shown that the uracil DNA glycosylases physically interacts with the PCNA-like sliding clamp in *Pyrobaculum aerophilum* (Yang et al. 2002) and in *S. solfataricus* (Dionne and Bell 2005). This interaction could be responsible for the recruitment of these and other DNA repair enzymes at the replication fork in vivo. However, our attempts failed to detect a direct physical interaction between Sso DNA pol Y1 and any of the three *S. solfataricus* PCNA-like homologs by surface plasmon resonance experiments suggesting that this interaction is not stable enough to be detected by this technique. Analysis of the physical and/or functional interaction between the *S. solfataricus* DNA pols and the enzymes responsible for repairing deaminated bases in DNA removal will provide insights into genome maintenance mechanisms in this hyper-thermophilic crenarchaeon.

Acknowledgments This work was supported by grants from ATIBB—BioTekNet. Centro Regionale di Competenza in Biotecnologie Industriali and from Agenzia Spaziale Italiana (Progetto MoMa n. 1/014/06/0). Authors are grateful to Dr Li Huang (Beijing, China) for the generous gift of the plasmid expressing His-tagged Sso DNA pol B1 in *E. coli*.

References

Asami Y, Murakami M, Shimizu M, Pisani FM, Hayata I, Nohmi T (2006) Visualization of the interaction between archaeal DNA polymerase and uracil-containing DNA by atomic force microscopy. Genes Cells 11:3–11

Blanco L, Bernad A, Blasco MA, Salas M (1991) A general structure for DNA-dependent DNA polymerases. Gene 108:165

Chung JH, Im EK, Park HY, Kwon JH, Lee S, Oh J, Hwang KC, Lee JH, Yang Y (2003) A novel uracil-DNA glycosylase family related to the helix-hairpin-helix DNA glycosylase superfamily. Nucleic Acids Res 31:2045–2055

Dionne I, Bell SD (2005) Characterization of an archaeal family 4 uracil DNA glycosylase and its interaction with PCNA and chromatin proteins. Biochem J 387:859–863

Fogg MJ, Pearl LH, Connolly BA (2002) Structural basis for uracil recognition by archaeal family B DNA polymerases. Nat Struct Biol 9:922–927

Friedberg EC, Wagner R, Radman M (2002) Specialized DNA polymerases, cellular survival, and the genesis of mutations. Science 296:1627–1630

Greagg MA, Fogg MJ, Panayotou G, Evans SJ, Connolly BA, Pearl LH (1999) A read-ahead function in archaeal DNA polymerases detects promutagenic template-strand uracil. Proc Natl Acad Sci USA 96:9045–9050

Grogan DW, Carver GT, Drake JW (2001) Genetic fidelity under harsh conditions: analysis of spontaneous mutation in the thermoacidophilic archaeon *Sulfolobus acidocaldarius*. Proc Natl Acad Sci USA 98:7928–7933

Gruz P, Shimizu M, Pisani FM, De Felice M, Kanke Y, Nohmi T (2003) Processing of DNA lesions by archaeal DNA polymerases from *Sulfolobus solfataricus*. Nucleic Acids Res 31:4024–4030

Gruz P, Pisani FM, Shimizu M, Yamada M, Hayashi I, Morikawa K, Nohmi T (2001) Synthetic activity of Sso DNA polymerase Y1, an archaeal DinB-like DNA polymerase, is stimulated by processivity factors proliferating cell nuclear antigen and replication factor C. J Biol Chem 276:47394–47401

Guo C, Fischhaber PL, Luk-Paszyc MJ, Masuda Y, Zhou J, Kamiya K, Kisker C, Friedberg EC (2003) Mouse Rev1 protein interacts with multiple DNA polymerases involved in translesion DNA synthesis. EMBO J 22:6621–6630

Kulaeva OI, Koonin EV, McDonald JP, Randall SK, Rabinovich N, Connaughton JF, Levine AS, Woodgate R (1996) Identification of a DinB/UmuC homolog in the archaeon *Sulfolobus solfataricus*. Mutat Res 357:245–253

Lasken RS, Schuster DM, Rashtchian A (1996) Archaebacterial DNA polymerases tightly bind uracil-containing DNA. J Biol Chem 271:17692–17696

Lindahl T (1993) Instability and decay of the primary structure of DNA. Nature 362:709–715

Lindahl T, Nyberg B (1974) Heat-induced deamination of cytosine residues in deoxyribonucleic acid. Biochemistry 13:3405–3410

Ling H, Boudsocq F, Woodgate R, Yang W (2001) Crystal structure of a Y-family DNA polymerase in action: a mechanism for error-prone and lesion-bypass replication. Cell 107:91–102

Lou H, Duan Z, Huo X, Huang L (2004) Modulation of hyperthermophilic DNA polymerase activity by archaeal chromatin proteins. J Biol Chem 279:127–132

Nohmi T (2006) Environmental stress and lesion-bypass DNA polymerases. Annu Rev Microbiol 60:231–253

Ohashi E, Murakumo Y, Kanjo N, Akagi J, Masutani C, Hanaoka F, Ohmori H (2004) Interaction of hREV1 with three human Y-family DNA polymerases. Genes Cells 9:523–531

Pisani FM, Rossi M (1994) Evidence that an archaeal alpha-like DNA polymerase has a modular organization of its associated catalytic activities. J Biol Chem 269:7887–7892

Pisani FM, Manco G, Carratore V, Rossi M (1996) Domain organization and DNA-induced conformational changes of an archaeal family B DNA polymerase. Biochemistry 35:9158–9166

Sartori AA, Jiricny J (2003) Enzymology of base excision repair in the hyperthermophilic archaeon *Pyrobaculum aerophilum*. J Biol Chem 278:24563–24576

Savino C, Federici L, Johnson KA, Vallone B, Nastopoulos V, Rossi M, Pisani FM, Tsernoglou D (2004) Insights into DNA replication: the crystal structure of DNA polymerase B1 from the archaeon *Sulfolobus solfataricus*. Structure 12:2001–2008

Shimizu M, Gruz P, Kamiya H, Kim SR, Pisani FM, Masutani C, Kanke Y, Harashima H, Hanaoka F, Nohmi T (2003) Erroneous incorporation of oxidized DNA precursors by Y-family DNA polymerases. EMBO Rep 4:269–273

Silvian LF, Toth EA, Pham P, Goodman MF, Ellenberger T (2001) Crystal structure of a DinB family error-prone DNA polymerase from *Sulfolobus solfataricus*. Nat Struct. Biol 8:984–989

Wang Z (2001) Translesion synthesis by the UmuC family of DNA polymerases. Mutat Res 486:59–70

Yang H, Chiang JH, Fitz-Gibbon S, Lebel M, Sartori AA, Jiricny J, Slupska MM, Miller JH (2002) Direct interaction between uracil-DNA glycosylase and a proliferating cell nuclear antigen homolog in the crenarchaeon Pyrobaculum aerophilum. J Biol Chem 277:22271–22278

Zhou BL, Pata JD, Steitz TA (2001) Crystal structure of a DinB lesion bypass DNA polymerase catalytic fragment reveals a classic polymerase catalytic domain. Mol Cell 8:427–437

Efficient and Erroneous Incorporation of Oxidized DNA Precursors by Human DNA Polymerase η

Masatomi Shimizu, Petr Gruz, Hiroyuki Kamiya, Chikahide Masutani, Yan Xu, Yukio Usui, Hiroshi Sugiyama, Hideyoshi Harashima, Fumio Hanaoka, and Takehiko Nohmi

Division of Genetics and Mutagenesis, National Institute of Health Sciences, Tokyo, Japan, Faculty of Pharmaceutical Sciences, Hokkaido University, Sapporo, Japan, Graduate School of Frontier Biosciences, Osaka University and SORST, JST, Osaka, Japan, Institute of Biomedical and Bioengineering, Tokyo Medical and Dental University, Tokyo, Japan, and Division of Medical Nutrition, Tokyo Healthcare University, Tokyo, Japan

Biochemistry®

Reprinted from
Volume 46, Number 18, Pages 5515–5522

Efficient and Erroneous Incorporation of Oxidized DNA Precursors by Human DNA Polymerase η[†]

Masatomi Shimizu,[‡,§] Petr Gruz,[‡] Hiroyuki Kamiya,[∥] Chikahide Masutani,[⊥] Yan Xu,[#] Yukio Usui,[▽] Hiroshi Sugiyama,[#,○] Hideyoshi Harashima,[∥] Fumio Hanaoka,[⊥] and Takehiko Nohmi*[,‡]

Division of Genetics and Mutagenesis, National Institute of Health Sciences, Tokyo, Japan, Faculty of Pharmaceutical Sciences, Hokkaido University, Sapporo, Japan, Graduate School of Frontier Biosciences, Osaka University and SORST, JST, Osaka, Japan, Institute of Biomedical and Bioengineering, Tokyo Medical and Dental University, Tokyo, Japan, and Division of Medical Nutrition, Tokyo Healthcare University, Tokyo, Japan

Received October 30, 2006; Revised Manuscript Received February 4, 2007

ABSTRACT: Altered oxidative metabolism is a property of many tumor cells. Oxidation of DNA precursors, i.e., dNTP pool, as well as DNA is a major source of mutagenesis and carcinogenesis. Here, we report the remarkable nature of human DNA polymerase η that incorporates oxidized dNTPs into a nascent DNA strand in an efficient and erroneous manner. The polymerase almost exclusively incorporated 8-hydroxy-dGTP (8-OH-dGTP) opposite template adenine (A) at 60% efficiency of normal dTTP incorporation, and incorporated 2-hydroxy-dATP (2-OH-dATP) opposite template thymine (T), guanine (G), or cytosine (C) at substantial rates. The synthetic primers having 8-hydroxy-G paired with template A or 2-hydroxy-A paired with template T, G, or C at the termini were efficiently extended. In contrast, human DNA polymerase ι incorporated 8-OH-dGTP opposite template A with much lower efficiency and did not incorporate 2-OH-dATP opposite any of the template bases. It did not extend the primers having the oxidized bases at the termini either. We propose that human DNA polymerase η may participate in oxidative mutagenesis through the efficient and erroneous incorporation of oxidized dNTPs during DNA synthesis.

Reactive oxygen species (ROS[1]), such as superoxide, hydrogen peroxide, hydroxyl radicals, and singlet oxygen, are produced through normal cellular metabolism, and formation of such radicals is further enhanced by irradiation or chemical exposure (*1*, *2*). ROS generates a variety of altered purines and pyrimidines in DNA (*3*, *4*), and oxidation of DNA plays important roles in mutagenesis, carcinogenesis, and aging (*5*, *6*). Several lines of evidence indicate, however, that oxidation of DNA precursors in the nucleotide pool, i.e., dNTPs, is another important cause of genome instability (*7*−*9*). Indeed, the frequency of A:T-to-C:G transversion mutations increases more than 1000-fold over the wild-type level in *Escherichia coli mutT* mutants, which are deficient in the ability to hydrolyze oxidized dGTP, i.e., 7,8-dihydro-8-oxo-dGTP (8-hydroxy-dGTP, 8-OH-dGTP, Figure 1A) (*10*, *11*). 8-OH-dGTP leads to A:T-to-C:G mutations when it is incorporated opposite adenine (A) in the template DNA because the incorporated 8-OH-G in DNA can pair with incoming dCMP in the next round of DNA replication (*8*, *12*). The high spontaneous A:T-to-C:G mutations in the *mutT* strain are almost completely suppressed when the *mutT* cells are cultured in anaerobic conditions, indicating the essential role of oxygen in the mutagenesis (*13*). Another oxidized nucleotide, i.e., 1,2-dihydro-2-oxo-dATP (2-hydroxy-dATP, 2-OH-dATP, Figure 1B), can induce G:C-to-T:A transversions when it is incorporated opposite guanine (G) in the template (*14*, *15*). The sanitizing enzyme, i.e., Orf135, in *E. coli* degrades 2-OH-dATP, and G:C-to-T:A mutations occur in the *orf135*-deficient strain more frequently than in the wild-type strain (*16*, *17*).

Oxidized dNTPs also cause genome instability in mammalian cells. Spontaneous tumorigenesis in mice deficient in *Mth1*, a mammalian counterpart of *mutT*, is much enhanced in lung, liver, and stomach, and the MTH1 protein hydrolyzes both 8-OH-dGTP and 2-OH-dATP (*18*, *19*). Recent studies with mismatch repair defective cells suggest that the majority of mutations in human cells that are deficient in mismatch repair functions do not arise from spontaneous replication errors, but from the incorporation of oxidized dNTPs (*20*, *21*). Thus, it is of great interest in

[†] The work was supported by grants-in-aid for Basic Research from the Ministry of Education, Culture, Sports, Science and Technology, Japan (to T.N. and M.S.) and from the Ministry of Health, Labour and Welfare, Japan, for Cancer Research from the Ministry of Health, Labour and Welfare, Japan and for International Collaborative Research from the Japan Health Science Foundation (SH34407).

* To whom correspondence should be addressed. Phone:+81-3-3700-9873. Fax: +81-3-3707-6950. E-mail: nohmi@nihs.go.jp.

[‡] National Institute of Health Sciences.

[§] Present address: Tokyo Healthcare University.

[∥] Hokkaido University.

[⊥] Osaka University.

[#] Tokyo Medical and Dental University.

[▽] Tokyo Healthcare University.

[○] Present address: Department of Chemistry, Graduate School of Science, Kyoto University, Kyoto, Japan.

[1] Abbreviations: ROS, reactive oxygen species; 8-OH-dGTP, 7,8-dihydro-8-oxo-dGTP; A, adenine; 2-OH-dATP, 1,2-dihydro-2-oxo-dATP; G, guanine; Pols, DNA polymerases; C, cytosine; TLS, translesion DNA synthesis; T, thymine; Polη, DNA polymerase η; Polι, DNA polymerase ι; HPLC, high performance liquid chromatography.

10.1021/bi062238r CCC: $37.00
Published on Web 04/18/2007

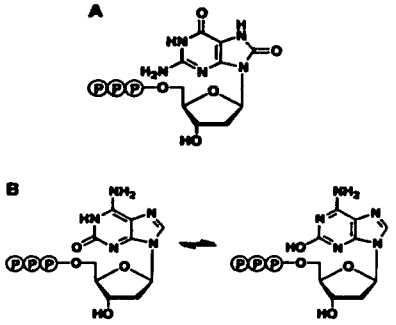

FIGURE 1: Structures of 8-OH-dGTP (A) and 2-OH-dATP (B). P represents a phosphate group.

the mechanisms as to how these oxidized dNTPs induce genome instability and oxidative carcinogenesis.

When the oxidized dNTPs escape from the sanitation by the enzymes, they will be incorporated into nascent DNA by DNA polymerases (Pols). However, oxidized dNTPs are in general poor substrates for Pols (*22*). For example, the efficiency of incorporation of 8-OH-dGTP by Polδ is more than 10^4-fold lower than that of incorporation of normal dGTP, and the enzyme prefers to incorporate 8-OH-dGTP opposite template cytosine (C) (*23*). 8-OH-dGTP is poorly incorporated into DNA by T7 Pol exo$^-$, HIV reverse transcriptase, *E. coli* Pol II, and Klenow exo$^-$ as well (*24*). An exception may be human Polβ, which incorporates 8-OH-dGTP into DNA with an efficiency of 10−20% of normal dGTP incorporation and favors its incorporation opposite template A (*25*). 2-OH-dATP is also a poor substrate for mammalian Pols. The efficiencies of incorporation of 2-OH-dATP opposite template T and C by Polα are more than 100-fold and 1000-fold, respectively, lower than those of incorporation of normal dATP and dGTP (*26*).

The Y-family Pols are recently recognized Pols that comprise proteins from different species, including members of Archaea, Bacteria, and Eukarya (*27*). The most distinct feature of this family of enzymes is their ability to bypass various lesions, such as ultraviolet light photoproducts, in template DNA (*28*−*30*). Some bypass reactions, i.e., translesion DNA synthesis (TLS), catalyzed by these enzymes are error prone while others are error free (*31*). Thus, this family of Pols seems to be involved in mutagenesis and DNA-damage tolerance (*32*). Interestingly, some of the Y-family Pols are shown to incorporate oxidized dNTPs into DNA in an erroneous manner. Archaeal Y-family Pols from *Sulfolobus* sp. and a bacterial Y-family Pol, i.e., DNA Pol IV (DinB) of *E. coli*, almost exclusively incorporate 8-OH-dGTP opposite template A, and 2-OH-dATP opposite template G and thymine (T) (*33*, *34*). Further genetic analysis with *E. coli sodfur* mutants suggests that both Y-family Pols of *E. coli*, i.e., Pol IV and Pol V (UmuD'C), are involved in oxidative mutagenesis caused by oxidized dNTPs (*34*). The enzymes may participate in sequential biochemical steps, such as incorporation of oxidized dNTPs into DNA and extension of primers having oxidized bases at the termini. Pol IV is also shown to be involved in induction of G:C-to-T:A mutations when 2-OH-dATP is directly introduced into *E. coli* cells by $CaCl_2$ treatment (*35*). Collectively, these results led us to postulate that certain human Y-family Pols might be involved in oxidative mutagenesis through incorrect and efficient incorporation of oxidized dNTPs into nascent DNA. In fact, human Polη incorporates oxidized dNTPs into DNA in an erroneous manner like the archaeal and bacterial Y-family Pols (*33*).

In this study, we quantitatively compared two human Y-family Pols, i.e., Polη and Polι, in the specificity and efficiency of incorporation of 8-OH-dGTP and 2-OH-dATP into a nascent DNA strand. Surprisingly, Polη incorporated 8-OH-dGTP opposite template A at almost the same efficiency as incorporation of normal dTTP, and incorporated 2-OH-dATP opposite template T, G, and C at substantial rates. In contrast, Polι poorly incorporated 8-OH-dGTP opposite template A and did not incorporate 2-OH-dATP opposite any of the bases in template DNA. Since Polη is constitutively associated with replication factories (*36*, *37*) and involved in multiple DNA transactions (*38*−*40*), we propose that this enzyme may be involved in mutagenesis through the efficient and erroneous incorporation of oxidized dNTPs into DNA strand.

EXPERIMENTAL PROCEDURES

Materials. Human Polη and Polι were purified as described (*41*, *42*). 8-OH-dGTP and 2-OH-dATP were prepared as described (*26*, *43*), and no discernible impurities were detected by high performance liquid chromatography (HPLC). dNTPs (ultrapure grade) were purchased from GE Healthcare Bio-Sciences KK (Tokyo).

DNA Substrates. Oligonucleotides containing 8-OH-G and 2-OH-A were prepared by the phosphoramidite method on controlled pore glass supports (1 μmol) by using a Beckman OLIGO1000 DNA synthesizer. After automated synthesis, the oligomers were detached from the support, deprotected, and purified by HPLC. The oligomers were identified by complete digestion of the oligomers with alkaline phosphatase and P1 nuclease to 2'-deoxymononucleosides. Other oligonucleotides were purchased from BEX Corp. (Tokyo). A Cy3-labeled 18-mer primer (5'-CGCGCGAAGACCG-GTTAC-3') or Cy3-labeled 19-mer primers (5'-CGCGC-GAAGACCGGTTACN-3' where N represents either 8-OH-G or 2-OH-A) were annealed to 36-mer templates (5'-GAAGGGATCCTTAAGACXGTAACCGGTCTTCGCGCG-3' where X represents A, C, G, or T) at a molar ratio of 1:1 to generate substrates. The 5'-Cy3-primer/templates generated by annealing the 18-mer primer to the 36-mer template were named substrate 1, and those generated by annealing the 19-mer primer having 8-OH-G or 2-OH-A to the 36-mer templates were named substrate 2 or 3, respectively. In control reactions, Cy3-labeled 19-mer primers (5'-CGCGC-GAAGACCGGTTACN-3' where N represents either G or A) were annealed to the 36-mer templates. The 5'-Cy3-primer/templates generated by annealing the 19-mer primer having G or A to the 36-mer templates were named substrate 4 or 5, respectively.

Steady-State Kinetic Analyses. The standard reaction mixtures (10 μL) contained 40 mM Tris-HCl (pH 8.0), 5 mM $MgCl_2$, 10 mM dithiothreitol, 250 μg/mL bovine serum albumin, 60 mM KCl, 2.5% glycerol, 1 nM Polη or Polι, 100 nM primer/template DNA (substrate 1, 2, or 3), and a single oxidized dNTP (8-OH-dGTP or 2-OH-dATP) or normal dNTP (dATP, dTTP, dGTP, or dCTP). The activity of Polι was also measured in the same reaction mixtures but without KCl (*44*). In that case, the concentration of $MgCl_2$ was reduced to 1 mM instead of 5 mM. Six different

concentrations of oxidized dNTP or normal dNTP were used to determine the kinetic parameters, i.e., k_{cat} and K_m (see below). The mixtures were incubated at 37 °C, and the reactions were terminated by adding 10 μL of stop solution (98% formamide, 10 mM EDTA, 10 mg/mL Blue Dextran). After heat denaturation for 10 min at 100 °C, the samples were separated by electrophoresis with 15% denaturing polyacrylamide gel containing 8 M urea and visualized by the Molecular Imager FX Pro System (Bio-Rad Laboratories, CA).

When the kinetic parameters for incorporation of oxidized or normal dNTPs into DNA were determined, the reaction mixtures contained substrate 1. The reaction time and the concentrations of oxidized dNTP and normal dNTP varied depending on the rates of reactions and the K_m values. For example, the incubation time was 1 min and the concentrations of 8-OH-dGTP varied from 0.05 to 10 μM for the analysis of incorporation of 8-OH-dGTP opposite template A by Polη. Identical reaction conditions were used for the analyses of incorporation of a single normal dNTP opposite a template canonical base by Polη. On the other hand, the incubation time was 10 min and the range of concentrations of 8-OH-dGTP was 5 to 100 μM to determine the parameters for incorporation of 8-OH-dGTP opposite template A by Polι. For the kinetic analyses of extension of primers having oxidized bases at the 3′-termini by Polη, the incubation time was 5 min and the concentrations of dGTP varied from 0.05 to 10 μM with the template/primer DNAs of substrate 2 or 3.

Data Analyses. Gel band intensities were measured using the Molecular Imager FX Pro System and Quantity One software (Bio-Rad Laboratories, CA), and nucleotide incorporation parameters were determined (*45*). Less than 20% of the primers were extended in these steady-state kinetic analyses, ensuring single-hit kinetics (*46*). For each DNA substrate, the rate of incorporation was plotted as a function of dNTP concentration, and the V_{max} and K_m values were determined by nonlinear regression fitting using the SigmaPlot software (Systat Software Inc., CA). k_{cat} was calculated by dividing V_{max} by the enzyme concentration. The fidelity of incorporation, i.e., F_{inc}, was calculated using the equation $F_{inc} = (k_{cat}/K_m)_{incorrect}/(k_{cat}/K_m)_{correct}$. All values are means ± standard errors from three experiments.

RESULTS

Efficient and Erroneous Incorporation of 8-OH-dGTP and 2-OH-dATP into DNA by Polη. Human Polη almost exclusively incorporates 8-OH-dGTP opposite template A and incorporates 2-OH-dATP opposite template T, G, and C (*33*). To compare two human Y-family Pols, we at first examined the specificity of human Polι incorporating 8-OH-dGTP and 2-OH-dATP into DNA. To this end, we used substrate 1 having four different bases in the N position in the template and incubated it with Polι in the presence of either 8-OH-dGTP or 2-OH-dATP. For the incorporation of 8-OH-dGTP, the primer annealed to the template strand having A in the N position was elongated, and no other primers annealed to templates having C, G, or T in the N position were extended (Figure 2A). These results indicate that Polι almost exclusively incorporates 8-OH-dGTP opposite template A as in the case of Polη. For the incorporation of 2-OH-dATP, no primers were elongated regardless of the bases in the template strand (Figure 2B). The activity of Polι is enhanced by omission of KCl from the reaction mixtures (*44*). We conducted, therefore, the experiments in the absence of KCl. Although the activity was enhanced several times (Table 1), the specificity was unchanged. 8-OH-dGTP was almost exclusively incorporated opposite template A, and no 2-OH-dATP was incorporated into DNA regardless of the template bases (data not shown). In control reactions, Polι incorporated normal dGTP opposite template C and T and incorporated normal dATP opposite template T and slightly opposite template C (Figure 2C,D). Thus, we conclude that, although the incorporation of 8-OH-dGTP opposite template A is a common feature to Y-family Pols, the specificity incorporating 2-OH-dATP into DNA is markedly distinct even within two human homologues.

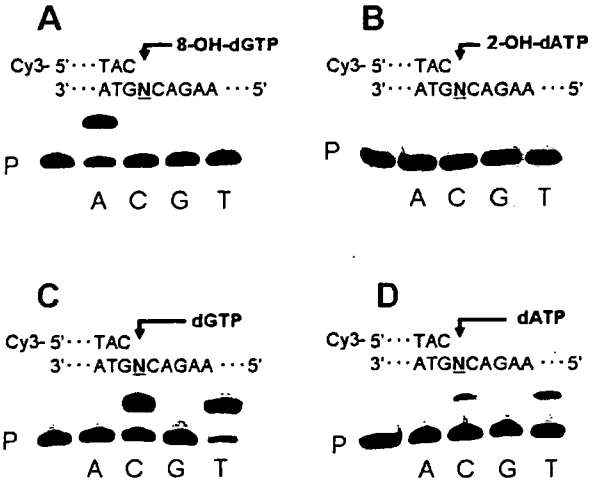

FIGURE 2: Incorporation of 8-OH-dGTP (A), 2-OH-dATP (B), dGTP (C), and dATP (D) into DNA by Polι. For analysis of incorporation of oxidized dNTPs (A and B), the reaction mixtures described in Experimental Procedures contained 1 nM Polι, 50 μM either 8-OH-dGTP or 2-OH-dATP, and 100 nM substrate 1. No normal dNTPs were included. For analysis of incorporation of normal dNTPs (C and D), the reaction mixtures contained 5 nM Polι, 50 μM either dGTP or dATP, and 100 nM substrate 1. In the reaction, KCl was omitted from the reaction mixtures and the concentration of $MgCl_2$ was 1 mM. The mixtures were incubated for 15 min at 37 °C, and the samples were processed as described in Experimental Procedures. The N in the template strand represents A, C, G, or T.

Table 1: Kinetic Parameters for Incorporation of 8-OH-dGTP and 2-OH-dATP by Polη and Polι

Pol	template base/ dNTP	K_m (μM)	k_{cat} (min^{-1})	k_{cat}/K_m (mM^{-1} min^{-1})	F_{inc}
Polη	A/dTTP	3.8 ± 0.52	15.4 ± 0.82	4.1	1
	A/8-OH-dGTP	4.2 ± 0.35	10.1 ± 0.35	2.4	0.59
	C/dGTP	1.2 ± 0.22	1.9 ± 0.1	1.6	1
	C/8-OH-dGTP	22.5 ± 8.3	0.3 ± 0.05	0.013	0.008
	C/dGTP	1.2 ± 0.22	1.9 ± 0.1	1.6	1
	C/2-OH-dATP	1.7 ± 0.55	0.1 ± 0.007	0.06	0.038
	G/dCTP	1.6 ± 0.12	9.5 ± 0.22	5.9	1
	G/2-OH-dATP	3.6 ± 0.6	0.35 ± 0.02	0.1	0.017
	T/dATP	5.2 ± 0.47	15 ± 0.61	2.9	1
	T/2-OH-dATP	3.0 ± 0.52	0.55 ± 0.03	0.18	0.062
Polι	A/dTTP	14.4 ± 3.0	5.1 ± 0.67	0.35	1
	A/8-OH-dGTP	132 ± 45.4	1.4 ± 0.31	0.011	0.031
	A/dTTP[a]	0.86 ± 0.14[a]	2.24 ± 0.08[a]	2.6[a]	1[a]
	A/8-OH-dGTP[a]	48.5 ± 7.37[a]	2.17 ± 0.15[a]	0.045[a]	0.017[a]

[a] The activities were measured without KCl in the reaction mixtures.

To compare the efficiency of two Pols for the incorporation of oxidized dNTPs quantitatively, we determined the steady-state kinetic parameters, i.e., K_m and k_{cat} (Table 1). The most remarkable feature of the kinetic data is the high efficiency of Polη incorporating 8-OH-dGTP opposite template A. The K_m and k_{cat} values (4.2 μM and 10.1 min^{-1}, respectively) were similar to those of incorporation of normal dTTP opposite template A (3.8 μM and 15.4 min^{-1}, respectively). Thus, the F_{inc}, i.e., $(k_{cat}/K_m)_{8\text{-OH-dGTP}}/(k_{cat}/K_m)_{dTTP}$, was about 0.6 (=2.4/4.1), which suggests that Polη incorporates 8-OH-dGTP opposite template A with the efficiency of about 60% of that of incorporation of normal dTTP. In addition, the incorporation of 8-OH-dGTP by Polη was strongly biased opposite template A compared to template C. The k_{cat}/K_m value of incorporation of 8-OH-dGTP opposite template A was more than 180 times greater than that of incorporation of 8-OH-dGTP opposite template C (2.4 versus 0.013). In contrast, Polι incorporates 8-OH-dGTP opposite template A with much lower efficiency. The k_{cat}/K_m value of incorporation of 8-OH-dGTP opposite template A was more than 200 and 30 times, respectively, less than that of incorporation of 8-OH-dGTP opposite template A by Polη (0.011 versus 2.4) and normal dTTP by Polι (0.011 versus 0.35). The k_{cat}/K_m value of incorporation of normal dTTP and 8-OH-dGTP opposite template A by Polι was enhanced several times by omission of KCl from the reaction mixtures (0.35 versus 2.6 and 0.011 versus 0.045). Nevertheless, the k_{cat}/K_m value of incorporation of 8-OH-dGTP opposite template A was more than 50 times less than that of incorporation of 8-OH-dGTP opposite template A by Polη (0.045 versus 2.4) and normal dTTP by Polι (0.045 versus 2.6).

We then determined the kinetic parameters of incorporation of 2-OH-dATP opposite template C, G, or T by Polη (Table 1). We did not determine the parameters for Polι because the enzyme did not incorporate 2-OH-dATP into DNA (Figure 2B). The K_m values for the incorporation of 2-OH-dATP by Polη were indistinguishable from those for the incorporation of normal dNTPs opposite template C, G, or T. However, the k_{cat} values for the incorporation of 2-OH-dATP were 20 to 30 times less than those of incorporation of normal dNTPs. Nevertheless, the F_{inc} values, i.e., $(k_{cat}/K_m)_{2\text{-OH-dATP}}/(k_{cat}/K_m)_{dNTP}$, opposite template C, G, and T were 0.038, 0.017, and 0.062, respectively, suggesting that Polη incorporates 2-OH-dATP opposite multiple template bases (except for A) with efficiency of 2 to 6% of that of incorporation of normal dNTPs. The order of k_{cat}/K_m values of incorporation of 2-OH-dATP opposite template bases was T (0.18) > G (0.10) > C (0.06).

Efficient Extension of Primers Having 8-OH-G or 2-OH-A at the 3′-Termini by Polη. To investigate whether Polη and Polι can extend the primers upon incorporation of oxidized dNTPs during DNA synthesis, we examined whether these Pols extend primers having either 8-OH-G or 2-OH-A at the 3′-termini. We annealed the primers to the template strands where the terminal oxidized base was paired with template A, C, G, or T and incubated the primer/templates, i.e., substrate 2 or 3, with Polη or Polι in the presence of four normal dNTPs. Polη extended the primer having 8-OH-G when the terminal oxidized base was paired with template A or C (Figure 3A). Virtually no extension was observed, however, when the terminal 8-OH-G was paired with template G or T. Polη could also extend primers having

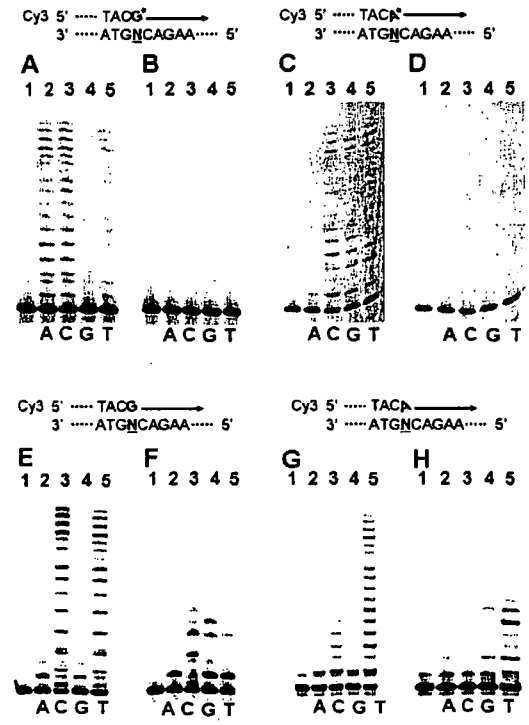

FIGURE 3: Extension of primers having 8-OH-G or 2-OH-A at the termini by Polη and Polι. Primers having 8-OH-G were extended by Polη (A) or Polι (B), and those having 2-OH-A were extended by Polη (C) or Polι (D). As control reactions, primers having G were extended by Polη (E) or Polι (F) and those having A were extended by Polη (G) or Polι (H). The reaction mixtures described in Experimental Procedures contained 1 nM Polη (A and C) or Polι (B and D), 200 μM four normal dNTPs (dATP, dCTP, dGTP, and dTTP), and 100 nM substrate 2 (A and B) or substrate 3 (C and D). The reaction mixtures were incubated for 5 min at 37 °C. In control reactions, the reaction mixtures contained 10 nM Polη (E and G) or Polι (F and H), 200 μM four normal dNTPs, and 100 nM substrate 4 (E and F) or substrate 5 (G and H). In control reactions with Polι (F and H), KCl was omitted from the reaction mixtures and the concentration of $MgCl_2$ was 1 mM. The reaction mixtures were incubated for 5 min (E and G) or 15 min (F and H) at 37 °C. The samples were processed as described in Experimental Procedures. Lane 1 (the leftmost lane) represents the position of the primers alone. The N in the template strands represents A (lane 2), C (lane 3), G (lane 4), and T (lane 5).

2-OH-A when the terminal oxidized base was paired with template C, G, or T (Figure 3C). In contrast, Polι was unable to extend any primers containing either 8-OH-G or 2-OH-A at the termini regardless of the pairing template bases (Figure 3B,D). In control reactions, Polη extended the primers having G at the termini when the terminal base was paired with template C or T (Figure 3E) and extended the primers having A at the termini when the terminal base was paired with template T (Figure 3G). Weak extension was observed when the terminal A was paired with template C. Polι was a poor extender even without oxidized bases at the termini of primers. It weakly extended primers when the terminal G or A was paired with canonical template bases (Figure 3F,H). These results suggest that Polη extends the primers upon incorporation of 8-OH-dGTP opposite template A or C, and extends the primers upon incorporation of 2-OH-dATP opposite template C, G, or T. Two Y-family Pols are distinct for their ability to extend the primers having oxidized bases at the termini.

We then determined the steady-state kinetic parameters for the extension, i.e., incorporation of next dGTP opposite

Table 2: Kinetic Parameters for Incorporation of dGTP with Primers Having Terminal 8-OH-G or 2-OH-A Pairing with Multiple Template Bases by Polη[a]

Template base/dNTP	K_m (μM)	k_{cat} (min^{-1})	k_{cat}/K_m (μM^{-1}min^{-1})
dGTP G*• A C	0.98±0.11	2.4±0.08	2.4
dGTP G*• C C	2.5±0.38	2.6±0.14	1.0
dGTP A*• C C	7.3±0.89	9.9±0.61	1.4
dGTP A*• G C	6.9±1.3	7.3±0.7	1.1
dGTP A*• T C	2.8±0.25	8.9±0.28	3.2

[a] G* = 8-OH-G; A* = 2-OH-A.

template C, by Polη from the primers having either 8-OH-G or 2-OH-A at the 3′-termini (Table 2). We did not determine the parameters for Polι because it did not extend the primers having 8-OH-G or 2-OH-A (Figure 3B,D).The terminal 8-OH-G in the primer was paired with template A or C while the terminal 2-OH-A was paired with template C, G, or T. The primer/templates, i.e., substrates 2 or 3, were incubated with Polη in the presence of dGTP without other dNTPs. For the extension from the primer having 8-OH-G at the termini, Polη extended the primer more efficiently when the terminal oxidized base was paired with template A than template C. The K_m value for the extension from the primer having 8-OH-G paired with template A was 2.5 times less than that for the extension from the primer having the oxidized base paired with template C (0.98 versus 2.5 μM) although the k_{cat} values were very similar between the two substrates (2.4 versus 2.6 min^{-1}). Thus, the ratio, i.e., $(k_{cat}/K_m)_{8\text{-OH-G:A}}/(k_{cat}/K_m)_{8\text{-OH-G:C}}$, was calculated to be 2.4 (=2.4/1.0), suggesting that Polη more than two times more efficiently extends the primer having 8-OH-G paired with template A compared to that having 8-OH-G paired with template C. For the extension from the primer having 2-OH-A at the 3′-temini, Polη extended the primer most efficiently when the oxidized base was paired with template T followed by template C and template G. The K_m value for the extension from the primer having 2-OH-A paired with template T (2.8 μM) was 2 to 3 times less than those for the extension from the primers having 2-OH-A paired with template G or template C (6.9 or 7.3 μM), and the k_{cat} values were not very different among the three substrates (8.9, 7.3, or 9.9 min^{-1}). Thus, the ratio of k_{cat}/K_m values, i.e., $(k_{cat}/K_m)_{2\text{-OH-A:T}}:(k_{cat}/K_m)_{2\text{-OH-A:G}}:(k_{cat}/K_m)_{2\text{-OH-A:C}}$, was 1: 0.34: 0.44, which suggests that Polη extends the primers having terminal 2-OH-A paired with template G or C at rates of 30 to 40% of that of extension from the primer having 2-OH-A paired with template T.

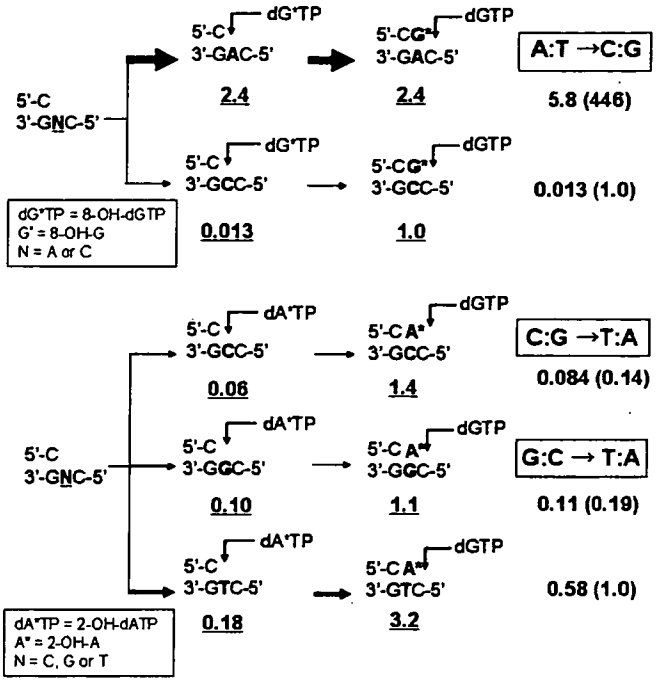

FIGURE 4: Total catalytic efficiency of incorporation of 8-OH-dGTP and 2-OH-dATP into DNA and the following primer extension by Polη. The total efficiency of incorporation and extension was calculated as the product of the individual k_{cat}/K_m values, e.g., 2.4 × 2.4 = 5.8 for the incorporation of 8-OH-dGTP opposite template A and the extension by incorporation of normal dGTP opposite template C. The individual k_{cat}/K_m value for each step is underlined. Relative efficiency is presented in parentheses. The relative values were calculated by setting the efficiency of incorporation of 8-OH-dGTP opposite template C and the following extension or incorporation of 2-OH-dATP opposite template T and the following extension as 1.0.

DISCUSSION

Oxidation is a major cause of spontaneous DNA damage that may contribute to mutagenesis, carcinogenesis, and aging (*5*, *6*). Oxidative damage in DNA is caused not only by direct oxidation of bases in DNA but also by incorporation of oxidized dNTPs in the nucleotide pool into DNA during chromosome replication (*7*, *47*). In this study, we have revealed the remarkable nature of Polη that incorporates 8-OH-dGTP opposite template A almost as efficiently as the incorporation of normal dTTP (Table 1). In addition, Polη extends the primer having 8-OH-G paired with template A more than two times more efficiently than the same primer having 8-OH-G paired with template C (Table 2). Calculation of the total efficiency by multiplying the individual k_{cat}/K_m values suggests that Polη prefers template A more than 400 times (446 = 5.8/0.013) to template C for the incorporation and extension (Figure 4). The efficient and erroneous incorporation of 8-OH-dGTP and the following extension may lead to A:T-to-C:G transversions because the incorporated 8-OH-G opposite template A may pair with dCMP in the next round of DNA replication (*8*, *43*, *48*). Besides 8-OH-dGTP, Polη incorporates 2-OH-dATP opposite template T, G, and C with efficiency of 2 to 6% of that of incorporation of normal dNTPs (Table 1). The F_{inc} values of incorporation of 2-OH-dATP opposite template T and C are about 20 and 50 times higher than the corresponding values by calf thymus Polα (*26*). Moreover, Polη can extend the primers having terminal 2-OH-A paired with template T, G, and C

(Figure 3, Table 2). The relative preference of Polη to template T:G:C for incorporation and extension is calculated as 1:0.19:0.14 (Figure 4). Incorporation of 2-OH-dATP opposite template G or C and the following extension may lead to G:C-to-T:A and C:G-to-T:A mutations since the incorporated 2-OH-A can pair with dTMP during the next round of DNA replication (*14*, *49*). Thus, we suggest that Polη has a potential to enhance mutagenesis through the efficient and erroneous incorporation of 8-OH-dGTP and 2-OH-dATP and the following extension during DNA replication (see below). It is possible, however, that other Pols may be involved in extension steps once oxidized dNTPs are inserted into nascent DNA by Polη.

Although Polη was initially identified as an error-free bypass Pol across a *cis-syn* thymine−thymine dimer in DNA (*28*, *29*), it appears to play important roles in several DNA transactions besides TLS (*50*). Polη interacts with RAD51 and has an activity to extend D loop, which is an intermediate of homologous recombination (*38*, *39*). It also participates in mutagenesis at A:T base pairs in immunoglobulin genes during somatic hypermutation (*40*). In addition, Polη is identified in replication factories in cells not deliberately exposed to DNA damaging agents (*36*, *37*), suggesting that it might constitutively gain access to the genomic DNA and contribute to mutagenesis and/or damage avoidance even without external DNA damage. Interestingly, *E. coli* Y-family Pols, i.e., Pol IV (DinB) and variants of Pol V (UmuD′C), are shown to be involved in the chromosome replication when the cells are treated with hydroxyurea, which does not induce DNA damage but depletes the nucleotide pool (*51*). In this case, the Y-family Pols appear to rescue the stalled replication by efficient incorporation of dNTPs in the depleted nucleotide pool at the expense of increased mutations. By analogy, we envisage that Polη might be localized in replication factories even without external DNA damage and contribute to rescue the stalled replication by incorporation of oxidized dNTPs when the nucleotide pool is heavily oxidized and/or the ratio of oxidized versus normal dNTPs is substantially enhanced. The replicative Pols might have difficulty to extend the primers without Polη in the situation since the oxidized dNTPs are generally difficult substrates for replicative Pols. However, the incorporation by Polη is erroneous and thus may induce mutations as described above. In fact, the mutagenicity of 8-OH-dGTP directly incorporated into human cells is reduced significantly when the expression of Polη is suppressed by RNAi technique (Kamiya et al., unpublished results). It is demonstrated that both 8-OH-dGTP and 2-OH-dATP are significant contributors to mutations in mismatch-repair-defective cells and incorporation of oxidized DNA precursors is a significant influence on microsatellite instability in repair-defective human tumor cells (*21*). We suggest, therefore, that Polη may be involved in mutagenesis by the incorporation of oxidized dNTPs in various DNA transactions when the nucleotide pool is oxidized and imbalanced.

Unlike Polη, Polι has a limited ability to incorporate oxidized dNTPs and extend the primers having the oxidized bases at the termini. It could not incorporate 2-OH-dATP into DNA and extend the primers having 8-OH-G or 2-OH-A regardless of the template bases under the experimental conditions (Figure 2B, Figure 3B,D). The only activity we could detect in this study was the incorporation of 8-OH-dGTP opposite template A (Figure 2A, Table 1). Polι is known to form Hoogsteen base pairing in the active site where the template A is rotated to the *syn* conformation while the incoming dTTP is in the *anti* conformation (*52*). Thus, the template A may be driven to the *syn* conformation when 8-OH-dGTP is incorporated. The Hoogsteen base pairing, i.e., template A (*syn*):8-OH-dGTP (*syn* or *anti*), may be the basis for the limited catalysis of incorporation of 8-OH-dGTP opposite template A. Nevertheless, Polι could not extend the primers having 8-OH-G at the termini. This may resemble the situation where Polι fails to further elongate the primers upon incorporation of C or T opposite 1,N^2-propano-2′-deoxyguanosine, which forms a *syn* conformation in the template DNA strand (*53*). Although it is possible that other Pols such as Polκ may help the extension step upon incorporation of 8-OH-G opposite template A by Polι, it seems unlikely that Polι is heavily involved in oxidative mutagenesis through the incorporation of oxidized dNTPs into nascent DNA.

In this study, we have revealed the remarkable nature of Polη that incorporates 8-OH-dGTP and 2-OH-dATP into DNA in an efficient and erroneous manner. We assume that the incoming 8-OH-dGTP adopts the *syn* conformation in the active site of Polη, which allows the formation of Hoogsteen base pairing with the *anti* form of template A. The active site large enough to accommodate bulky DNA adducts may permit the *syn* conformation of incoming 8-OH-dGTP, which is favored when it pairs with A in a DNA duplex (*54*). The Hoogsteen base pairing, i.e., 8-OH-dGTP (*syn*) and template A (*anti*), which might be opposite to the conformation of pairing bases in the active site of Polι, could be the basis for the efficient and erroneous incorporation of 8-OH-dGTP by Polη. Interestingly, yeast and human Polη can bypass 8-OH-G in DNA in an efficient but error-free manner by insertion of dCMP opposite the oxidized base in the template strand (*55*). In these cases, the large active site of Polη is thought to allow the *anti* conformation of 8-OH-G in the template strand, which introduces barriers for other Pols (*56*). Since oxidative damage in the nucleotide pool as well as DNA is a major source of spontaneous mutagenesis and carcinogenesis, the present study warrants the validity of further research on the roles of Polη in the oxidative mutagenesis in human cells.

ACKNOWLEDGMENT

We thank Dr. Roger Woodgate at National Institutes of Health (Bethesda, MD) for a generous gift of Polι and for helpful discussion. The work is supported by grants-in-aid from the Ministry of Education, Culture, Sports, Science and Technology, Japan, the Ministry of Health, Labour and Welfare, Japan, and the Japan Health Science Foundation.

REFERENCES

1. Ames, B. N., and Gold, L. S. (1991) Endogenous mutagens and the causes of aging and cancer, *Mutat. Res. 250*, 3−16.
2. Henle, E. S., and Linn, S. (1997) Formation, prevention, and repair of DNA damage by iron/hydrogen peroxide, *J. Biol. Chem. 272*, 19095−19098.
3. Bjelland, S., and Seeberg, E. (2003) Mutagenicity, toxicity and repair of DNA base damage induced by oxidation, *Mutat. Res. 531*, 37−80.
4. Kamiya, H. (2003) Mutagenic potentials of damaged nucleic acids produced by reactive oxygen/nitrogen species: approaches using

synthetic oligonucleotides and nucleotides: survey and summary, *Nucleic Acids Res. 31*, 517−531.
5. Ames, B. N. (1983) Dietary carcinogens and anticarcinogens. Oxygen radicals and degenerative diseases, *Science 221*, 1256−1264.
6. Jackson, A. L., and Loeb, L. A. (2001) The contribution of endogenous sources of DNA damage to the multiple mutations in cancer, *Mutat. Res. 477*, 7−21.
7. Sekiguchi, M., and Tsuzuki, T. (2002) Oxidative nucleotide damage: consequences and prevention, *Oncogene 21*, 8895−8904.
8. Michaels, M. L., and Miller, J. H. (1992) The GO system protects organisms from the mutagenic effect of the spontaneous lesion 8-hydroxyguanine (7,8-dihydro-8-oxoguanine), *J. Bacteriol. 174*, 6321−6325.
9. Nakabeppu, Y., Sakumi, K., Sakamoto, K., Tsuchimoto, D., Tsuzuki, T., and Nakatsu, Y. (2006) Mutagenesis and carcinogenesis caused by the oxidation of nucleic acids, *Biol. Chem. 387*, 373−379.
10. Maki, H., and Sekiguchi, M. (1992) MutT protein specifically hydrolyses a potent mutagenic substrate for DNA synthesis, *Nature 355*, 273−275.
11. Yanofsky, C., Cox, E. C., and Horn, V. (1966) The unusual mutagenic specificity of an *E. coli* mutator gene, *Proc. Natl. Acad. Sci. U.S.A. 55*, 274−281.
12. Kasai, H. (2002) Chemistry-based studies on oxidative DNA damage: formation, repair, and mutagenesis, *Free Radical Biol. Med. 33*, 450−456.
13. Sakai, A., Nakanishi, M., Yoshiyama, K., and Maki, H. (2006) Impact of reactive oxygen species on spontaneous mutagenesis in *Escherichia coli*, *Genes Cells 11*, 767−778.
14. Inoue, M., Kamiya, H., Fujikawa, K., Ootsuyama, Y., Murata-Kamiya, N., Osaki, T., Yasumoto, K., and Kasai, H. (1998) Induction of chromosomal gene mutations in *Escherichia coli* by direct incorporation of oxidatively damaged nucleotides. New evaluation method for mutagenesis by damaged DNA precursors in vivo, *J. Biol. Chem. 273*, 11069−11074.
15. Kamiya, H., and Kasai, H. (2000) 2-Hydroxy-dATP is incorporated opposite G by *Escherichia coli* DNA polymerase III resulting in high mutagenicity, *Nucleic Acids Res. 28*, 1640−1646.
16. Kamiya, H., Iida, E., Murata-Kamiya, N., Yamamoto, Y., Miki, T., and Harashima, H. (2003) Suppression of spontaneous and hydrogen peroxide-induced mutations by a MutT-type nucleotide pool sanitization enzyme, the *Escherichia coli* Orf135 protein, *Genes Cells 8*, 941−950.
17. Kamiya, H., Murata-Kamiya, N., Iida, E., and Harashima, H. (2001) Hydrolysis of oxidized nucleotides by the *Escherichia coli* Orf135 protein, *Biochem. Biophys. Res. Commun. 288*, 499−502.
18. Tsuzuki, T., Egashira, A., Igarashi, H., Iwakuma, T., Nakatsuru, Y., Tominaga, Y., Kawate, H., Nakao, K., Nakamura, K., Ide, F., Kura, S., Nakabeppu, Y., Katsuki, M., Ishikawa, T., and Sekiguchi, M. (2001) Spontaneous tumorigenesis in mice defective in the MTH1 gene encoding 8-oxo-dGTPase, *Proc. Natl. Acad. Sci. U.S.A. 98*, 11456−11461.
19. Fujikawa, K., Kamiya, H., Yakushiji, H., Fujii, Y., Nakabeppu, Y., and Kasai, H. (1999) The oxidized forms of dATP are substrates for the human MutT homologue, the hMTH1 protein, *J. Biol. Chem. 274*, 18201−18205.
20. Colussi, C., Parlanti, E., Degan, P., Aquilina, G., Barnes, D., Macpherson, P., Karran, P., Crescenzi, M., Dogliotti, E., and Bignami, M. (2002) The mammalian mismatch repair pathway removes DNA 8-oxodGMP incorporated from the oxidized dNTP pool, *Curr. Biol. 12*, 912−918.
21. Russo, M. T., Blasi, M. F., Chiera, F., Fortini, P., Degan, P., Macpherson, P., Furuichi, M., Nakabeppu, Y., Karran, P., Aquilina, G., and Bignami, M. (2004) The oxidized deoxynucleoside triphosphate pool is a significant contributor to genetic instability in mismatch repair-deficient cells, *Mol. Cell Biol. 24*, 465−474.
22. Nohmi, T., Kim, S. R., and Yamada, M. (2005) Modulation of oxidative mutagenesis and carcinogenesis by polymorphic forms of human DNA repair enzymes, *Mutat. Res. 591*, 60−73.
23. Einolf, H. J., and Guengerich, F. P. (2001) Fidelity of nucleotide insertion at 8-oxo-7,8-dihydroguanine by mammalian DNA polymerase δ. Steady-state and pre-steady-state kinetic analysis, *J. Biol. Chem. 276*, 3764−3771.
24. Einolf, H. J., Schnetz-Boutaud, N., and Guengerich, F. P. (1998) Steady-state and pre-steady-state kinetic analysis of 8-oxo-7,8-dihydroguanosine triphosphate incorporation and extension by replicative and repair DNA polymerases, *Biochemistry 37*, 13300−13312.
25. Miller, H., Prasad, R., Wilson, S. H., Johnson, F., and Grollman, A. P. (2000) 8-oxodGTP incorporation by DNA polymerase β is modified by active-site residue Asn279, *Biochemistry 39*, 1029−1033.
26. Kamiya, H., and Kasai, H. (1995) Formation of 2-hydroxydeoxyadenosine triphosphate, an oxidatively damaged nucleotide, and its incorporation by DNA polymerases. Steady-state kinetics of the incorporation, *J. Biol. Chem. 270*, 19446−19450.
27. Ohmori, H., Friedberg, E. C., Fuchs, R. P., Goodman, M. F., Hanaoka, F., Hinkle, D., Kunkel, T. A., Lawrence, C. W., Livneh, Z., Nohmi, T., Prakash, L., Prakash, S., Todo, T., Walker, G. C., Wang, Z., and Woodgate, R. (2001) The Y-family of DNA polymerases, *Mol. Cell 8*, 7−8.
28. Masutani, C., Kusumoto, R., Yamada, A., Dohmae, N., Yokoi, M., Yuasa, M., Araki, M., Iwai, S., Takio, K., and Hanaoka, F. (1999) The *XPV* (xeroderma pigmentosum variant) gene encodes human DNA polymerase η, *Nature 399*, 700−704.
29. Johnson, R. E., Prakash, S., and Prakash, L. (1999) Efficient bypass of a thymine-thymine dimer by yeast DNA polymerase, Polη, *Science 283*, 1001−1004.
30. Prakash, S., Johnson, R. E., and Prakash, L. (2005) Eukaryotic translesion synthesis DNA polymerases: specificity of structure and function, *Annu. Rev. Biochem. 74*, 317−353.
31. Friedberg, E. C. (2005) Suffering in silence: the tolerance of DNA damage, *Nat. Rev. Mol. Cell Biol. 6*, 943−953.
32. Nohmi, T. (2006) Environmental Stress and Lesion-Bypass DNA Polymerases, *Annu. Rev. Microbiol. 60*, 231−253.
33. Shimizu, M., Gruz, P., Kamiya, H., Kim, S. R., Pisani, F. M., Masutani, C., Kanke, Y., Harashima, H., Hanaoka, F., and Nohmi, T. (2003) Erroneous incorporation of oxidized DNA precursors by Y-family DNA polymerases, *EMBO Rep. 4*, 269−273.
34. Yamada, M., Nunoshiba, T., Shimizu, M., Gruz, P., Kamiya, H., Harashima, H., and Nohmi, T. (2006) Involvement of Y-family DNA polymerases in mutagenesis caused by oxidized nucleotides in *Escherichia coli*, *J. Bacteriol. 188*, 4992−4995.
35. Satou, K., Yamada, M., Nohmi, T., Harashima, H., and Kamiya, H. (2005) Mutagenesis induced by oxidized DNA precursors: roles of Y family DNA polymerases in *Escherichia coli*, *Chem. Res. Toxicol. 18*, 1271−1278.
36. Kannouche, P., Broughton, B. C., Volker, M., Hanaoka, F., Mullenders, L. H., and Lehmann, A. R. (2001) Domain structure, localization, and function of DNA polymerase η, defective in xeroderma pigmentosum variant cells, *Genes Dev. 15*, 158−172.
37. Tissier, A., Kannouche, P., Reck, M. P., Lehmann, A. R., Fuchs, R. P., and Cordonnier, A. (2004) Co-localization in replication foci and interaction of human Y-family members, DNA polymerase polη and REVl protein, *DNA Repair (Amsterdam) 3*, 1503−1514.
38. McIlwraith, M. J., Vaisman, A., Liu, Y., Fanning, E., Woodgate, R., and West, S. C. (2005) Human DNA polymerase η promotes DNA synthesis from strand invasion intermediates of homologous recombination, *Mol. Cell 20*, 783−792.
39. Kawamoto, T., Araki, K., Sonoda, E., Yamashita, Y. M., Harada, K., Kikuchi, K., Masutani, C., Hanaoka, F., Nozaki, K., Hashimoto, N., and Takeda, S. (2005) Dual roles for DNA polymerase η in homologous DNA recombination and translesion DNA synthesis, *Mol. Cell 20*, 793−799.
40. Mayorov, V. I., Rogozin, I. B., Adkison, L. R., and Gearhart, P. J. (2005) DNA polymerase η contributes to strand bias of mutations of A versus T in immunoglobulin genes, *J. Immunol. 174*, 7781−7786.
41. Masutani, C., Kusumoto, R., Iwai, S., and Hanaoka, F. (2000) Mechanisms of accurate translesion synthesis by human DNA polymerase η, *EMBO J. 19*, 3100−3109.
42. Tissier, A., McDonald, J. P., Frank, E. G., and Woodgate, R. (2000) polι, a remarkably error-prone human DNA polymerase, *Genes Dev. 14*, 1642−1650.
43. Cheng, K. C., Cahill, D. S., Kasai, H., Nishimura, S., and Loeb, L. A. (1992) 8-Hydroxyguanine, an abundant form of oxidative DNA damage, causes G----T and A----C substitutions, *J. Biol. Chem. 267*, 166−172.
44. Vaisman, A., Frank, E. G., Iwai, S., Ohashi, E., Ohmori, H., Hanaoka, F., and Woodgate, R. (2003) Sequence context-dependent replication of DNA templates containing UV-induced lesions by human DNA polymerase ι, *DNA Repair (Amsterdam) 2*, 991−1006.

45. Creighton, S., Bloom, L. B., and Goodman, M. F. (1995) Gel fidelity assay measuring nucleotide misinsertion, exonucleolytic proofreading, and lesion bypass efficiencies, *Methods Enzymol. 262*, 232−256.
46. Goodman, M. F., Creighton, S., Bloom, L. B., and Petruska, J. (1993) Biochemical basis of DNA replication fidelity, *Crit. Rev. Biochem. Mol. Biol. 28*, 83−126.
47. Slupphaug, G., Kavli, B., and Krokan, H. E. (2003) The interacting pathways for prevention and repair of oxidative DNA damage, *Mutat. Res. 531*, 231−251.
48. Pavlov, Y. I., Minnick, D. T., Izuta, S., and Kunkel, T. A. (1994) DNA replication fidelity with 8-oxodeoxyguanosine triphosphate, *Biochemistry 33*, 4695−4701.
49. Satou, K., Harashima, H., and Kamiya, H. (2003) Mutagenic effects of 2-hydroxy-dATP on replication in a HeLa extract: induction of substitution and deletion mutations, *Nucleic Acids Res. 31*, 2570−2575.
50. Lehmann, A. R. (2006) New functions for Y family polymerases, *Mol. Cell 24*, 493−495.
51. Godoy, V. G., Jarosz, D. F., Walker, F. L., Simmons, L. A., and Walker, G. C. (2006) Y-family DNA polymerases respond to DNA damage-independent inhibition of replication fork progression, *EMBO J. 25*, 868−879.
52. Nair, D. T., Johnson, R. E., Prakash, S., Prakash, L., and Aggarwal, A. K. (2004) Replication by human DNA polymerase-iota occurs by Hoogsteen base-pairing, *Nature 430*, 377−380.
53. Wolfle, W. T., Johnson, R. E., Minko, I. G., Lloyd, R. S., Prakash, S., and Prakash, L. (2005) Human DNA polymerase ι promotes replication through a ring-closed minor-groove adduct that adopts a *syn* conformation in DNA, *Mol. Cell Biol. 25*, 8748−8754.
54. Kouchakdjian, M., Bodepudi, V., Shibutani, S., Eisenberg, M., Johnson, F., Grollman, A. P., and Patel, D. J. (1991) NMR structural studies of the ionizing radiation adduct 7-hydro-8-oxodeoxyguanosine (8-oxo-7H-dG) opposite deoxyadenosine in a DNA duplex. 8-Oxo-7H-dG(syn).dA(anti) alignment at lesion site, *Biochemistry 30*, 1403−1412.
55. Haracska, L., Yu, S. L., Johnson, R. E., Prakash, L., and Prakash, S. (2000) Efficient and accurate replication in the presence of 7,8-dihydro-8-oxoguanine by DNA polymerase η, *Nat. Genet. 25*, 458−461.
56. Carlson, K. D., and Washington, M. T. (2005) Mechanism of efficient and accurate nucleotide incorporation opposite 7,8-dihydro-8-oxoguanine by *Saccharomyces cerevisiae* DNA polymerase η, *Mol. Cell Biol. 25*, 2169−2176.

BI062238R

doi:10.1016/j.jmb.2008.01.033 J. Mol. Biol. (2008) xx, xxx–xxx

JMB

Available online at www.sciencedirect.com

ScienceDirect

ELSEVIER

Miscoding Properties of 2′-Deoxyinosine, a Nitric Oxide-Derived DNA Adduct, during Translesion Synthesis Catalyzed by Human DNA Polymerases

Manabu Yasui[1]*, Emi Suenaga[2], Naoki Koyama[1], Chikahide Masutani[3], Fumio Hanaoka[3], Petr Gruz[1], Shinya Shibutani[4], Takehiko Nohmi[1], Makoto Hayashi[1] and Masamitsu Honma[1]

[1]*Division of Genetics and Mutagenesis, National Institute of Health Sciences, 1-18-1 Kamiyoga, Setagaya, Tokyo 158-8501, Japan*

[2]*Division of Pharmacognosy, Phytochemistry and Narcotics, National Institute of Health Sciences, 1-18-1 Kamiyoga, Setagaya, Tokyo 158-8501, Japan*

[3]*Cellular Biology Laboratory, Graduate School of Frontier Biosciences, Osaka University, 1-3 Yamada-oka, Suita, Osaka 565-0871, Japan*

[4]*Department of Pharmacological Sciences, State University of New York at Stony Brook, Stony Brook, NY 11794-8651, USA*

Received 26 November 2007; received in revised form 10 January 2008; accepted 14 January 2008

Edited by J. Karn

Chronic inflammation involving constant generation of nitric oxide (•NO) by macrophages has been recognized as a factor related to carcinogenesis. At the site of inflammation, nitrosatively deaminated DNA adducts such as 2′-deoxyinosine (dI) and 2′-deoxyxanthosine are primarily formed by •NO and may be associated with the development of cancer. In this study, we explored the miscoding properties of the dI lesion generated by Y-family DNA polymerases (pols) using a new fluorescent method for analyzing translesion synthesis. An oligodeoxynucleotide containing a single dI lesion was used as a template in primer extension reaction catalyzed by human DNA pols to explore the miscoding potential of the dI adduct. Primer extension reaction catalyzed by pol α was slightly retarded prior to the dI adduct site; most of the primers were extended past the lesion. Pol η and pol κΔC (a truncated form of pol κ) readily bypassed the dI lesion. The fully extended products were analyzed by using two-phased PAGE to quantify the miscoding frequency and specificity occurring at the lesion site. All pols, that is, pol α, pol η, and pol κΔC, promoted preferential incorporation of 2′-deoxycytidine monophosphate (dCMP), the wrong base, opposite the dI lesion. Surprisingly, no incorporation of 2′-deoxythymidine monophosphate, the correct base, was observed opposite the lesion. Steady-state kinetic studies with pol α, pol η, and pol κΔC indicated that dCMP was preferentially incorporated opposite the dI lesion. These pols bypassed the lesion by incorporating dCMP opposite the lesion and extended past the lesion. These relative bypass frequencies past the dC:dI pair were at least 3 orders of magnitude higher than those for the dT:dI pair. Thus, the dI adduct is a highly miscoding lesion capable of generating A→G transition. This •NO-induced adduct may play an important role in initiating inflammation-driven carcinogenesis.

Keywords: inflammation; nitric oxide; DNA adduct; translesion synthesis; nonradioactive analysis

*Corresponding author. E-mail address: m-yasui@nihs.go.jp.

Abbreviations used: •NO, nitric oxide; dI, 2′-deoxyinosine; dX, 2′-deoxyxanthosine; dA, 2′-deoxyadenosine; 8-OxodG, 8-oxo-2′-deoxyguanosine; dNTP, 2′-deoxynucleoside triphosphate; Alexa546, Alexa Fluor 546 dye; pol α, human DNA polymerase α; pol η, human DNA polymerase η; pol κ, human DNA polymerase κ; pol κΔC, a truncated form of pol κ; F_{ins}, frequency of insertion; F_{ext}, frequency of extension; 8-NO_2-dG, 8-nitro-2′-deoxyguanosine; dCMP, 2′-deoxycytidine monophosphate; dTMP, 2′-deoxythymidine monophosphate; dTTP, 2′-deoxythymidine triphosphate; dCTP, 2′-deoxycytidine triphosphate; dGTP, 2′-deoxyguanosine triphosphate; Cy3, Cyanin 3; endo V, endonuclease V.

Introduction

Chronic inflammation involving constant generation of nitric oxide ($^{\bullet}NO$) by macrophages has been recognized as a factor related to carcinogenesis.[1–3] $^{\bullet}NO$ can attack neighboring epithelial and stromal cells by damaging the DNA, altering their genome stability. There are two possible major pathways for the $^{\bullet}NO$ reaction (Fig. 1). One pathway involves the combination of $^{\bullet}NO$ and superoxide with the formation of highly toxic peroxynitrite ($ONOO^-$). Spontaneous hydrolysis of peroxynitrite under physiological conditions generates secondary radical species ($^{\bullet}NO_2$, $^{\bullet}OH$, and $CO_3^{-\bullet}$) that induce oxidation and nitration of diverse DNA adducts[4,5] such as 8-oxo-2′-deoxyguanosine (8-OxodG) and 8-nitro-2′-deoxyguanosine (8-NO_2-dG).[6,7] A second involves nitrosative deamination of DNA base by $^{\bullet}NO$ via formation of several nitrosating agents, which predominantly exist as nitrous anhydride (N_2O_3) at physiological pH.[8] The DNA base products by nitrosative deamination mainly involve conversion of adenine to hypoxanthine [2′-deoxyinosine (dI)] (Fig. 2), guanine to xanthine [2′-deoxyxanthosine (dX)], and cytosine to uracil.[9–12]

The spectrum of nitrosative DNA adducts in N_2O_3-treated plasmid DNA was composed of approximately 2% dG–dG cross-links, 4–6% abasic sites, and 25–35% each of dI, dX, and 2′-deoxyuracyl.[12,13] Moreover, dI and dX, as well as lipid peroxidated adducts, were increased in the cellular DNA of tissues from the $^{\bullet}NO$-overproducing SJL mouse model of inflammation.[14] The increased production of $^{\bullet}NO$ was associated with an increased mutation frequency.[15] When human TK6 cells were exposed to $^{\bullet}NO$, the increase in mutation rates observed at hypoxanthineguanine phosphoribosyltransferase and thymidine kinase gene loci correlated with the 40-fold increase of dI and dX more than did that of the controls in the cellular DNA.[10] Thus, the dI adduct is one of the major $^{\bullet}NO$-derived DNA lesions and may contribute to the burden of carcinogenesis in inflammation tissue.

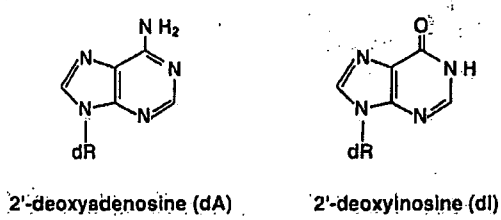

2′-deoxyadenosine (dA) 2′-deoxyinosine (dI)

Fig. 2. Structures of dA and dI adducts.

Site-specifically dI-modified oligodeoxynucleotides have been used as DNA templates for investigating the miscoding events using only mouse pol α and rat pol β.[16] The previous report showed that rat pol β inserted only 2′-deoxycytidine monophosphate (dCMP) opposite the dI lesion and that mouse pol α tended to incorporate dCMP and 2′-deoxythymidine monophosphate (dTMP) opposite the lesion. However, the miscoding events were investigated with the detection of mismatched base pairs by loss of a restriction enzyme recognition site. No quantitative analysis, therefore, has been performed for determination of miscoding events generated by dI.

Human DNA pol η[17] and pol κ[18,19] that are associated with translesion synthesis past a variety of DNA lesions[20,21] were examined. We have here explored the miscoding properties of the dI lesion that occurred during DNA replication catalyzed by

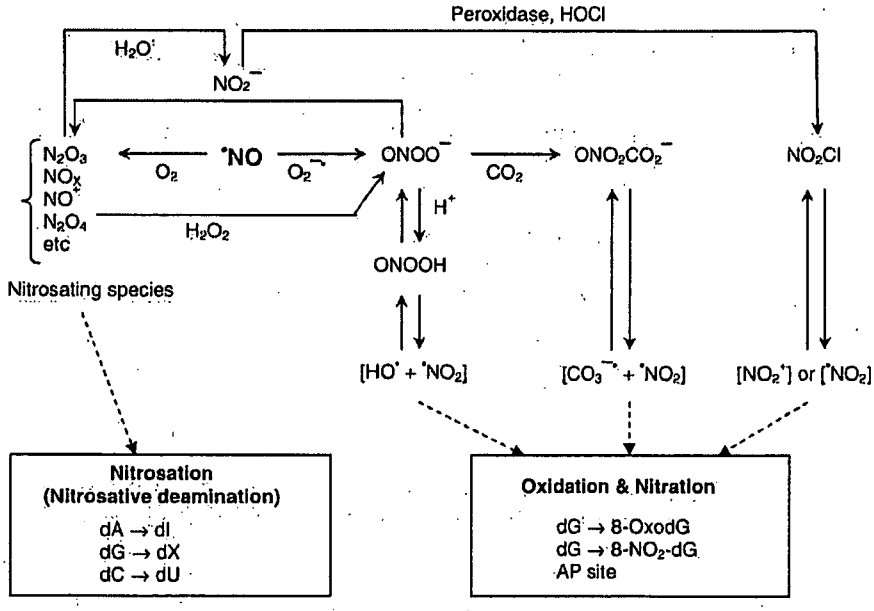

Fig. 1. Possible pathways for the formation of $^{\bullet}NO$-induced DNA adducts.

human DNA pols. In addition, instead of using radioisotope, we have developed a new fluorescent technique for analyzing translesion synthesis and quantifying the miscoding specificity and frequency using two-phased PAGE (Fig. 3).[22,23] Relative bypass frequencies past the dI lesion were also determined by steady-state kinetic studies.[24,25]

Results

Primer extension reactions catalyzed by human DNA pols on dI-modified DNA template

Using unmodified and dI-modified 38-mer templates, we conducted primer extension reactions in the presence of four 2′-deoxynucleoside triphosphates (dNTPs) and varying amounts of pol α, pol η, or pol κΔC (Fig. 4). Primer extension occurred rapidly on unmodified templates to form fully extended products. With the dI-modified template, primer extension catalyzed by pol α was slightly retarded one base before the lesion (see arrowhead in Fig. 4). However, when pol η or pol κΔC was used, primer extension resulted in fully extended products. No blockage was detected at the dI adduct site. When the amounts of pols were increased, products representing more than 32-mer bases long were produced on the unmodified and dI-modified templates. Blunt-end addition to the fully extended product (33–34-mers) was observed, as reported earlier for *Escherichia coli* and mammalian DNA pols.[26,27]

Miscoding frequencies and specificities of the dI adduct

Translesion synthesis catalyzed by pol α, pol η, or pol κΔC was conducted in the presence of all four dNTPs. The fully extended products (approximately 28–34-mers) past the unmodified or modified adducts were recovered, digested by EcoRI, and subjected to two-phased PAGE for quantitative analysis of base substitutions and deletions as described in Materials and Methods (Fig. 3). A standard mixture of six Alexa Fluor 546 dye (Alexa546)-labeled oligodeoxynucleotides containing dC, dA, dG, or dT opposite the lesion or one- and two-base deletions can be resolved by this method (Fig. 5). The percentage of 2′-deoxynucleoside monophosphate incorporation was normalized to the amount of the starting primer. When an unmodified dA template was used, expected incorporation of dTMP, the correct base, was observed opposite dA (Fig. 5). As indicated by the arrowhead in Fig. 5b, small amounts of unknown products were detected. When pol α was used with a template containing dI, dCMP (83.3% of the starting primers) was exclusively incorporated opposite the lesion. Similarly, pol η and pol κΔC promoted preferential incorporation of dCMP (55.0% and 74.7%, respectively) opposite the lesion. No deletions were detected. Surprisingly, no incorporation of dTMP, the correct base, was detected opposite the dI adduct with all pols, that is, pol α, pol η, and pol κΔC.

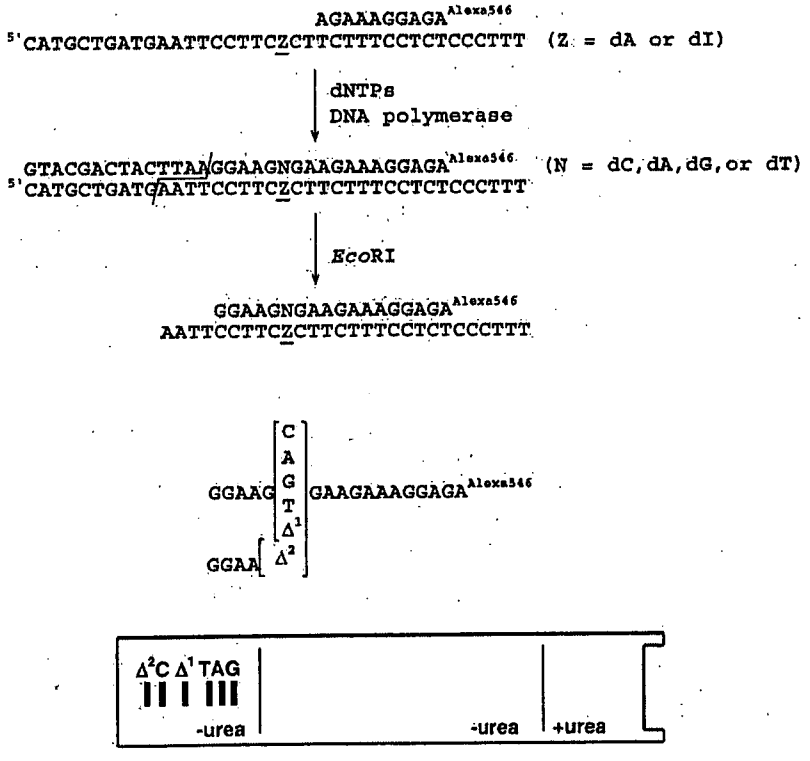

Fig. 3. Diagram of the fluorescent two-phased PAGE to determine miscoding specificity of DNA adducts. Unmodified and dI-modified 38-mer templates are annealed to either an Alexa546-labeled 10-mer primer or an Alexa546-labeled 12-mer primer. Primer extension reactions catalyzed by DNA pol α, pol η, or pol κΔC were conducted in the presence of four dNTPs. Fully extended products formed during DNA synthesis were recovered from the polyacrylamide gel (30×40×0.05 cm), annealed with a complementary 38-mer, cleaved with EcoRI, and subjected to a two-phased PAGE (20×65×0.05 cm), as described in Materials and Methods. To determine miscoding specificity, mobilities of the reaction products were compared with those of 18-mer standards containing dC, dA, dG, or dT opposite the lesion and one-base (Δ^1) or two-base (Δ^2) deletions.

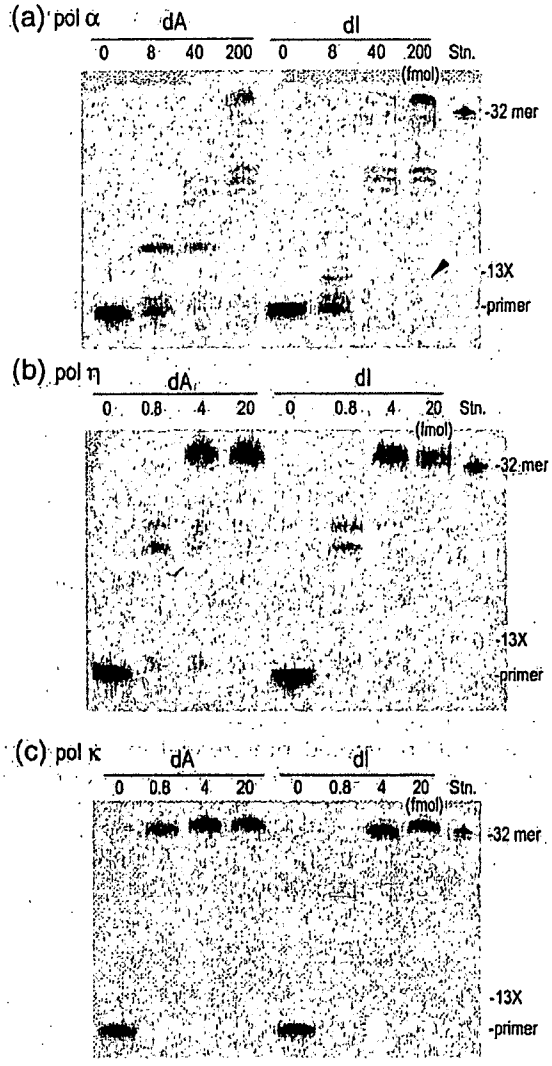

Fig. 4. Primer extension reactions catalyzed by pol α, pol η, or pol κΔC on dI-modified DNA template. Using unmodified or dI-modified 38-mer templates primed with an Alexa546-labeled 10-mer, we performed primer extension reactions at 25 °C for 30 min in a buffer containing four dNTPs (100 μM each) and varying amounts of (a) pol α (0, 8, 40, and 200 fmol), (b) pol η, or (c) pol κΔC (0, 0.8, 4, and 20 fmol), as described in Materials and Methods. The whole amount of the reaction mixture was subjected to 20% denaturing PAGE (30×40×0.05 cm). An Alexa546-labeled 32-mer (5′AGAGGAAAGTAGCGAAGGAATTCATCAGCATG) was used as a marker of fully extended product. 13X represents the adducted position.

Kinetic studies on dI-modified templates

Steady-state kinetic studies were performed using pol α, pol η, and pol κΔC to determine the frequency of dNTP incorporation (F_{ins}) opposite the dI lesion and chain extension (F_{ext}) from the primer terminus using the same sequence context that was used for the two-phased PAGE assay (Table 1). With pol α, the F_{ins} value for deoxythymidine triphosphate (dTTP) (1.21×10^{-2}), the correct base, opposite the dI was 59 times lower than that for 2′-deoxycytidine triphosphate (dCTP) (0.718). The relative bypass frequency ($F_{ins}\times F_{ext}$) past the dC:dI pair was approximately 2100 times higher than that for the dT:dI pair. F_{ins} and F_{ext} values for dA:dI and dG:dI were not detectable. When pol η was used, the F_{ins} value for dCTP (0.551), the wrong base, opposite the dI was 27 times higher than that for dTTP (2.07×10^{-2}) and was 17 and 75 times higher than that for 2′-deoxyadenosine triphosphate and 2′-deoxyguanosine triphosphate (dGTP), respectively. The F_{ext} value for the dC:dI pair was also higher than that for other 2′-deoxynucleoside monophosphates paired with dI. As a result, the $F_{ins}\times F_{ext}$ value past dC:dI was at least 3 orders of magnitude higher than that past other pairs. Similarly, with pol κ, $F_{ins}\times F_{ext}$ past dC:dI was much higher than that for other base pairs. F_{ins} and F_{ext} values for dTTP were 119 and 55 times lower than that for dCTP, respectively. Thus, all pols, that is, pol α, pol η, and pol κΔC, exclusively promote misincorporation of dCMP opposite the dI lesion during translesion synthesis, since $F_{ins}\times F_{ext}$ values of other dNTPs were considerably lower that that for dCTP, the wrong base.

Discussion

Primer extension reactions catalyzed by DNA pols are a powerful method to explore translesion synthesis past DNA adducts and their accompanying kinetic parameters of nucleotide insertion and extension. A ^{32}P-labeled oligodeoxynucleotide at the 5′-terminus is widely employed in such analyses; however, the handling of hazardous radioisotopes is intricate for use and waste disposal. Indeed, use of radioisotopes is restricted in many countries including Japan. As an alternative to ^{32}P, we used fluorescent dyes, Alexa546 and Cyanin 3 (Cy3), to label the 5′-terminus of the oligodeoxynucleotide used as primers and standard markers. The detection limits of Alexa546- and Cy3-labeled primers were approximately 120 and 240 times lower than that of the ^{32}P-labeled primer, respectively. However, when Alexa546-labeled primers (500 fmol) were annealed with DNA template (750 fmol) and the assays of primer extension and kinetic studies were carried out in this work, the resultant data were quantitative and reproducible (Figs. 6 and 7). Alexa546 exhibits a more sensitive and photostable fluorescence than Cy3. Moreover, even under repeated thawing and melting, an Alexa546-labeled oligomer stored at −20 °C was not degraded for at least 6 months. Using this method, we determined the miscoding frequency and specificity of 8-OxodG, which is known to generate predominantly 2′-deoxyadenosine monophosphate misincorporation at the lesion site. The results obtained from Alexa546 labeling were consistent with that from ^{32}P labeling (data not shown). Thus, Alexa546 was applicable to two-phased PAGE. Therefore, we have used this fluorescent method to explore translesion synthesis past dI adducts and its miscoding specificity and frequency using two-phased PAGE.

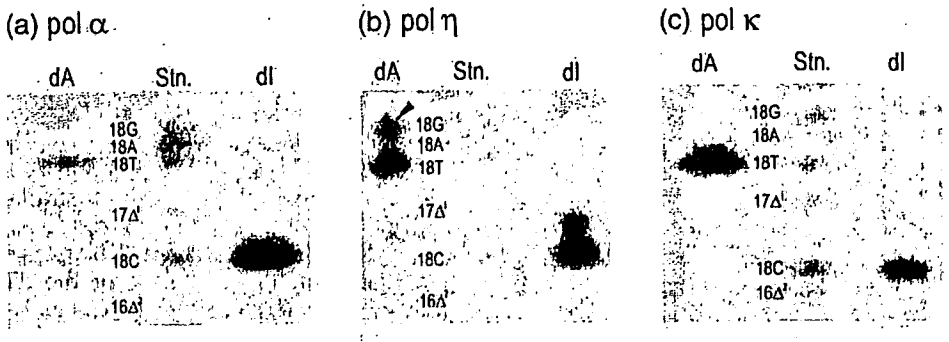

Fig. 5. Miscoding specificities of the dI lesion in reactions catalyzed by pol α, pol η, or pol κΔC. Using unmodified and dI-modified 38-mer templates primed with an Alexa546-labeled 12-mer, we conducted primer extension reactions at 25 °C for 30 min in a buffer containing four dNTPs (100 μM each) and either pol α (200 fmol for unmodified and dI-modified templates), pol κΔC, or pol η (20 fmol for unmodified and dI-modified templates), as described in Materials and Methods. The extended reaction products (>26 bases long) produced on the unmodified and dI-modified templates were extracted following PAGE. The recovered oligodeoxynucleotides were annealed to an unmodified 38-mer and cleaved with EcoRI restriction enzyme, as described in Materials and Methods. The entire product from the unmodified and dI-modified templates was subjected to two-phased PAGE (20×65×0.05 cm). Mobilities of reaction products were compared with those of 18-mer standards (Fig. 3) containing dC, dA, dG, or dT opposite the lesion and one-base (Δ^1) or two-base (Δ^2) deletions.

The mutation spectrum induced by •NO has been investigated in a variety of experimental systems. •NO gas showed mutagenicity in TK6 cells[10] and caused predominantly A:T→G:C transitions in plasmids replicated in cultured human and *E. coli* cells[28,29] and C→T transitions in a bacterial system.[9] Moreover, •NO-releasing compounds exclusively resulted in G:C→A:T transitions in pSP189 plasmids propagated in human cells.[30] Using similar •NO-releasing compounds, $ONOO^-$ caused G:C→T:A and G:C→C:G transversions with the same experimental system.[31,32] Thus, based on the information obtained from these previous reports, the mutation spectrum by •NO has not been extensively determined yet.[33] In our previous studies, the miscoding frequencies and specificities of dX, 8-NO_2-dG, and 8-OxodG lesions were quantitatively determined by two-phased PAGE. As a result, 8-NO_2-dG[34] and 8-OxodG[17,35] are miscoding lesions generating primarily G→T transversions (~20% and ~38%, respectively), while the miscoding spectrum of the dX adduct[36] exclusively shows G→A transitions (~50%), which differs from that of 8-NO_2-dG and 8-OxodG. This indicates that each DNA adduct has a unique miscoding specificity and frequency. The mutation spectrum by •NO can be hardly determined due to the presence of diverse

Table 1. Kinetic parameters for nucleotide insertion and chain extension reactions catalyzed by human DNA pol α, pol η, and pol κΔC

		Insertion dNTP			Extension dGTP			
		↓GAAGAAAGGAGA^{Alexa546} 5′CCTTCZCTTCTTTCCTCTCCCTTT			↓NGAAGAAAGGAGA^{Alexa546} 5′CCTTCZCTTCTTTCCTCTCCCTTT			
	N:Z	K_m (μM)[a]	V_{max} (% min^{-1})[a]	F_{ins}	K_m (μM)[a]	V_{max} (% min^{-1})[a]	F_{ext}	$F_{ins}\times F_{ext}$
Pol α	T:A	0.56±0.03	0.53±0.02	1.0	0.41±0.14	0.31±0.03	1.0	1.0
	C:Z	0.73±0.26	0.47±0.03	0.718	0.48±0.09	0.25±0.01	0.679	0.487
	A:Z	N.D.	N.D.	N.D.	N.D.	N.D.	N.D.	N.D.
	G:Z	N.D.	N.D.	N.D.	N.D.	N.D.	N.D.	N.D.
	T:Z	9.74±1.60	0.11±0.07	1.21×10^{-2}	7.09±1.50	10.1±0.65	1.92×10^{-2}	2.32×10^{-4}
Pol η	T:A	0.65±0.17	5.37±0.26	21.0	0.69±0.13	7.49±0.11	1.0	1.0
	C:Z	1.74±0.58	7.79±0.48	0.551	0.96±0.18	8.44±0.25	0.809	0.446
	A:Z	4.87±1.22	1.28±0.03	3.18×10^{-2}	6.63±0.76	2.66±0.08	3.66×10^{-2}	1.16×10^{-3}
	G:Z	16.1±1.03	1.00±0.01	7.30×10^{-3}	11.6±4.23	1.14±0.11	9.40×10^{-3}	6.86×10^{-5}
	T:Z	7.00±1.97	1.19±0.03	2.07×10^{-2}	6.76±0.41	4.99±0.02	6.72×10^{-2}	1.39×10^{-3}
Pol κΔC	T:A	1.43±0.38	11.1±0.47	1.0	0.55±0.07	13.9±0.54	1.0	1.0
	C:Z	1.36±0.40	10.3±0.44	0.987	0.79±0.76	13.1±0.12	0.651	0.642
	A:Z	15.5±4.30	1.10±0.05	9.23×10^{-3}	10.7±2.43	2.17±0.07	8.13×10^{-3}	7.50×10^{-5}
	G:Z	84.0±15.4	0.76±0.30	1.12×10^{-3}	12.8±2.25	0.51±0.05	1.57×10^{-3}	1.75×10^{-6}
	T:Z	23.5±6.93	1.50±0.11	8.26×10^{-3}	5.28±0.37	1.59±0.03	1.18×10^{-2}	9.74×10^{-5}

Kinetics of nucleotide insertion and chain extension reactions were determined as described in Materials and Methods. Frequencies of nucleotide insertion (F_{ins}) and chain extension (F_{ext}) were estimated by the following equation: $F=(V_{max}/K_m)_{[wrong\ pair]}/(V_{max}/K_m)_{[correct\ pair=dT:dA]}$. Z=dA or dI lesion.

N.D., not detectable.

[a] Data are expressed as mean±SD obtained from three independent experiments.

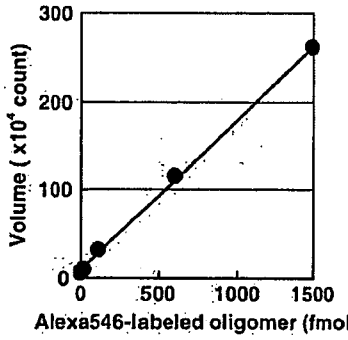

Fig. 6. Calibration curve using fluorescent oligomers labeled by Alexa546. Varying amounts of Alexa546-labeled oligomer were subjected to 20% denaturing PAGE. The volume of bands was quantitatively measured by using Molecular Imager FX Pro and Quantity One software (Bio-Rad) to find a linear range in the fluorescent analysis.

DNA adducts caused by ˙NO-involved species (Fig. 1) and its miscoding variety.[17,34,35] Therefore, the quantitative miscoding properties of each ˙NO-derived DNA adduct must be required to explore its roles in the inflammation-driven carcinogenesis.

The miscoding specificity of dI was determined by using an *in vitro* experimental system that can quantify base substitutions and deletions formed during replication in the presence of four dNTPs. Pol α, pol η, and pol κΔC incorporated dCMP (83.3%, 55.0%, and 74.7%, respectively) preferentially opposite the dI lesion rather than dTMP, the correct base (Fig. 5). Kamiya *et al.* reported earlier that mouse pol α inserted dCMP and dTMP, the correct base, opposite the dI lesion.[16] In contrast, human pol α promoted direct incorporation of dCMP only (Fig. 5). These indicate that the pols promote miscoding by incorporating dCMP opposite the dI lesion during DNA synthesis. Thus, dI is a highly miscoding lesion, generating A→G transitions in human cells. Steady-state kinetic studies supported these results. When pol α, pol η, and pol κΔC were used, $F_{ins} \times F_{ext}$ values for dC:dI pairs were 2100, 320, and 6600 times higher than those for dT:dI pairs, respectively (Table 1). Therefore, the kinetic results were consistent with that observed using two-phased PAGE analysis. Taken together, both analyses showed that human

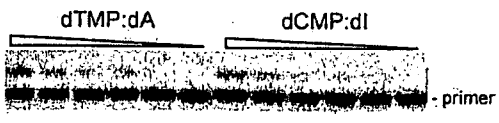

Fig. 7. Typical image of PAGE for kinetic studies performed by Alexa546 labeling. Using unmodified or dI-modified 38-mer templates (750 fmol) primed with an Alexa546-labeled 12-mer (500 fmol), we conducted primer extension reactions at 25 °C for 2 min in a buffer containing pol κΔC (1 fmol) and either dTTP (0.25–25 μM for unmodified templates) or dCTP (0.25–25 μM for dI-modified templates), as described in Materials and Methods. The whole amount of the reaction mixture was subjected to 20% denaturing PAGE (30×40×0.05 cm).

DNA pols miscode at dI lesions by exclusively incorporating dCMP. The miscoding specificity was consistent with that observed in *E. coli*,[9] mammalian cells,[10,37] and mice exposed to ˙NO.[15]

To compare the relative bypass frequency of dI, dX, and 8-NO_2-dG by pol α, pol η, and pol κΔC, these adducts were embedded in a similar sequence context[34,36] (Table 2). With pol α, the $F_{ins} \times F_{ext}$ ratio for the dC:dI/dT:dI pairs was 2100. This number was remarkably higher than that for the dT:dX/dC:dX (ratio=1.5) or dA:8-NO_2-dG/dC:8-NO_2-dG (ratio=0.01) pairs. Similar results were observed with pol η and pol κΔC. The ratios of $F_{ins} \times F_{ext}$ past dI were 2 orders of magnitude higher than those of dX and 8-NO_2-dG. Thus, dI adducts promote a higher miscoding potential (A→G transitions) than those of dX or 8-NO_2-dG. However, the highly mutagenic dI lesions did not show serious mutation frequency[9,10] even though they were predominantly paired with the wrong base, dCMP. Endonuclease V (endo V) has shown to be a dI-specific endonuclease.[38–40] Methylpurine glycosylase also recognizes this lesion.[41–43] For instance, *E. coli* cells lacking the endo V (*nfi*) gene were shown to exhibit elevated mutation frequencies when exposed to nitrous acid. The increased mutations were predominantly A:T→G:C mutations, followed by lesser G:C→A:T mutations.[44,45] This indicates that endo V is primarily involved in the repair of dI lesions.[44–48]

The structure of double-stranded oligodeoxynucleotide containing the dI:dC pair was determined by thermodynamic and NMR studies.[49,50] dI can most stably pair with dC among four dNs, and its geometric structure is similar in form with the Watson–Crick structure (Fig. 8). dI has a carbonyl group at position C6 and a positive charge at position N1 after dA suffers from nitrosative deamination by ˙NO. Thus, since the structure of dI is similar to that of dG rather than dA, the dI adduct can predominantly pair with dC, the wrong base.

In conclusion, nonradioactive kinetic studies and two-phased PAGE were performed to explore the

Table 2. $F_{ins} \times F_{ext}$ past DNA adducts by human DNA pol α, pol η, and pol κΔC

	Z=	dI[a]	dX[b]	8-NO_2-dG[c]
Pol α	C:Z	**0.487**	4.50×10^{-3}	1.69×10^{-3}
	A:Z	N.D.	2.18×10^{-4}	$\mathbf{1.31\times10^{-5}}$
	G:Z	N.D.	1.11×10^{-5}	2.63×10^{-6}
	T:Z	2.32×10^{-4}	$\mathbf{6.68\times10^{-3}}$	5.87×10^{-6}
Pol η	C:Z	**0.446**	5.24×10^{-2}	6.94×10^{-3}
	A:Z	1.16×10^{-3}	1.71×10^{-3}	$\mathbf{5.09\times10^{-3}}$
	G:Z	6.86×10^{-5}	2.94×10^{-4}	4.63×10^{-4}
	T:Z	1.39×10^{-3}	**0.259**	4.06×10^{-4}
Pol κΔC	C:Z	**0.642**	8.39×10^{-3}	6.37×10^{-5}
	A:Z	7.50×10^{-5}	2.43×10^{-6}	$\mathbf{2.88\times10^{-5}}$
	G:Z	1.75×10^{-6}	2.48×10^{-6}	2.62×10^{-6}
	T:Z	9.74×10^{-5}	$\mathbf{5.12\times10^{-2}}$	6.62×10^{-7}

Values in boldface show a primarily misincorporated base opposite the DNA adduct.
N.D., not detectable.
[a] Data were taken from Table 1.
[b] Data were taken from Ref. 36.
[c] Data were taken from Ref. 34.